5-28-1957

A Study of the Density and Molecular Species of Polonium and Tellurium Vapor

Angelo L. Giorgi

POLONIUM AND TELLURIUM VAPOR

GIORGI

MILLERS FALLS

ERASE

COTTON CONTENT

A STUDY OF THE DENSITY AND MOLECULAR SPECIES OF POLONIUM AND TELLURIUM VAPOR

By

Angelo L. Giorgi

A Thesis

In partial fulfillment of the Requirements

for the Degree of Doctor of Philosophy

The University of New Mexico

1957

This dissertation, directed and approved by the candidate's committee, has been accepted by the Graduate Committee of the University of New Mexico in partial fulfillment of the requirements for the degree of

DOCTOR OF PHILOSOPHY

E. L. Castetter

DEAN

May 28, 1957

DATE

Committee

Millard Kahn

CHAIRMAN

John H. Settle

J. L. Rebsomen

C. E. Bradt

M. J. Bowman

E. L. Madsen

A STUDY OF THE DENSITY AND MOLECULAR SPECIES OF POLONIUM AND TELLURIUM VAPOR

Acknowledgment

The writer desires to express his appreciation to Dr. Milton Kahn, Dr. Melvin Bowman, and Dr. Dwayne Vier for their assistance and helpful counsel during the pursuit of this study.

The work was performed at the Los Alamos Scientific Laboratory. The cooperation of Donald Cochran in the performance of the cyclotron irradiation of the arsenic and antimony targets and of Roby Bevan and Leonard Treiman in the performance of the calorimetric measurements of the polonium samples is gratefully acknowledged.

TABLE OF CONTENTS

PART		PAGE
I	INTRODUCTION	1
	Effect of Dissociation	4
	Thermodynamic Quantities	5
II	EXPERIMENTAL	7
	Description of Apparatus	7
	Temperature Measurement and Control	11
	Description of Method	13
	Effect of Decay	14
	Effect of Decay Products	15
	Preparation of Chemical Reagents	15
	Polonium	15
	Tellurium	27
	Selenium	31
	Analytical Reagents	35
	Preparation of Samples	35
	Preparation of Counting Standards	36
	Calibration of Volume of Quartz Cells	37
	Standardization of Thermocouples	37
	Analysis of Samples	38
	Polonium	38
	Tellurium	39
	Selenium	40
	Errors	40

III RESULTS AND CALCULATIONS 42

Treatment of Counting Data 43

Calculation of Vapor Density 46

Calculation of Molar Heat of Vaporization 46

Calculation of Vapor Pressure 47

Calculation of Normal Boiling Point 47

Calculation of Trouton's Constant 48

Calculation of Association Number 48

IV DISCUSSION 76

Variation of the (θT_A) Values with Temperature of Selenium Vapor 76

Molar Heat of Vaporization, Normal Boiling Point, and Trouton's Constant for Tellurium 78

Molar Heat of Vaporization, Normal Boiling Point, and Trouton's Constant for Polonium 82

Conclusion 93

BIBLIOGRAPHY 95

LIST OF FIGURES

FIGURE		PAGE
1.	Diagram of Differential Temperature Furnace and Counters Assembly	8
2.	Differential Temperature Furnace and Counters Assembly	9
3.	Quartz Cell and Metal Housing	10
4.	Heater and Thermocouple Circuits	12
5.	Distillation Apparatus	18
6.	Vacuum Line with Distillation Apparatus	19
7.	Distillation Apparatus and Oscillator Coil	20
8.	Dissolution Apparatus for Polonium	21
9.	Polonium Electrodeposition Set-up in Lucite Box	23
10.	Polonium Plating Cell	24
11.	Schematic Drawing of Automatic Plating Current Control	26
12.	Log (θT_A) versus $1/T_B$ for Selenium	55
13.	Log (θT_A) versus $1/T_B$ for Tellurium	59
14.	Log P versus $1/T_B$ for Tellurium	60
15.	Tellurium Data Fitted to Brooks Curve	61
16.	Log (θT_A) versus $1/T_B$ for Polonium with 0 to 1 Atomic Per Cent Lead	65
17.	Log P versus $1/T_B$ for Polonium with 0 to 1 Atomic Per Cent Lead	66

18. Calculated Data for Polonium Fitted to Brooks Curve 67

19. Log (θT_A) versus $1/T_B$ for Polonium with Various Lead Content 71

20. Log P versus $1/T_B$ for Polonium with Various Lead Content..... 72

21. Log P versus $1/T_B$ for Polonium with 3 to 3.5 Atomic Per Cent Lead 75

LIST OF TABLES

TABLE		PAGE
I	Experimental Data for Selenium, Run No. 1	50
II	Experimental Data for Selenium, Run No. 2	51
III	Experimental Data for Selenium, Run No. 3	52
IV	Experimental Data for Selenium, Run No. 4	53
V	Experimental Data for Selenium Vapor at Constant Pressure	54
VI	Experimental Data for Tellurium, Run No. 5	56
VII	Experimental Data for Tellurium, Run No. 6	57
VIII	Experimental Data for Tellurium Vapor at Constant Pressure	58
IX	Experimental Data for Polonium with 0 to 1 Atomic Per Cent Lead, Run No. 7	62
X	Experimental Data for Polonium with 0 to 1 Atomic Per Cent Lead, Run No. 8	63
XI	Experimental Data for Polonium Vapor at Constant Pressure	64
XII	Experimental Data for Polonium with 3 to 3.5 Atomic Per Cent Lead, Run No. 9	68
XIII	Experimental Data for Polonium with 17 to 17.8 Atomic Per Cent Lead, Run No. 10	69
XIV	Experimental Data for Polonium with 29 to 31 Atomic Per Cent Lead, Run No. 11	70
XV	Experimental Data for Polonium with 3 to 3.5 Atomic Per Cent Lead, Run No. 12	73

XVI Experimental Data for Polonium with 3 to 3.5 Atomic Per Cent Lead, Run No. 13 74

XVII Comparison of Values of Heat of Vaporization, Normal Boiling Point, and Trouton's Constant Reported for Tellurium 81

XVIII Comparison of Values of Heat of Vaporization, Normal Boiling Point, and Trouton's Constant Reported for Polonium 85

XIX Comparison of Calculated and Observed Values for the Decrease in Vapor Pressure of Polonium by Different Lead Concentrations..... 90

PART I

Introduction

The purpose of this investigation was to determine the nature of the species of polonium and tellurium in equilibrium in the vapor phase at temperatures ranging from 422° to 1013° C. for polonium and from 512° to 880° C. for tellurium. Such information was based on measurements of the variation of vapor pressure and vapor density with temperature. The results of this investigation suggest that both polonium and tellurium exist as diatomic molecules in the vapor phase over the aforementioned temperature ranges.

The variation of the vapor pressure of tellurium with temperature has been studied by several investigators. The earliest work was carried out by Doolan and Partington[1] using a gas-saturation method. They obtained values of 0.464, 3.34, and 14.1 mm., for measurements at 488°, 578°, and 671° C., respectively. Schneider and Schupp[2] used the same method with improvements over the range 8.15 to 67.2 mm. The vapor pressure above the solid was studied by Niawa and Sibata[3] between 0.045 and 0.887 mm. Recently Brooks[4], using a quartz bourdon gage, determined the vapor pressure of tellurium from 1.1 to 161 mm. over a temperature range from 515° to 832° C. Vapor density measurements for tellurium are reported only for temperatures above 1000° C.[5]

The vapor pressure of polonium has been determined by only one

investigator. Brooks[6], using a quartz bourdon gage, made measurements from 0.3 to 90 mm. over a temperature range from 438° to 745° C. The variation of the vapor density of polonium with temperature is not reported in the literature.

In the present study measurements of vapor density for polonium were made over a temperature range from 422° to 1013° C. The vapor density of tellurium was measured over a temperature range from 512° to 880° C. To test the sensitivity of the vapor density method for detecting dissociation in the vapor, measurements were also made on selenium from 308° to 729° C.

There are three general methods for measuring vapor density. They are: (1) the Dumas method[7] in which the weight of a known volume of vapor is determined; (2) the Hofmann method[8] in which the volume of vapor from a known weight of material is measured; and (3) the Victor Meyer method[9] in which the volume of air (or noble gas) displaced by the vaporization of a known weight of substance is determined. These methods are normally used at room temperature with material of fairly high vapor pressures. To adapt these methods for use at elevated temperatures with substances of low vapor pressures, various investigators have introduced several modifications. Sommaruga[10] used boiling sulfur in the Dumas method for the measurement of the vapor density of indigo at 444.6° C. Magnus and Schmid[11] modified the Hofmann method to obtain greater accuracy. Ramsay and Young[12] constructed a Hofmann-type apparatus in which the pressure and temperature could be varied in order to allow a series of measurements to be carried out with one sample up

to 250°C. The bulb of a Victor Meyer-type apparatus was heated in a paraffin bath by P. Blackman[13] in studies of the dissociation of phosphorus pentachloride at temperatures from 170° to 250°C. The molecular weight of hydrogen peroxide vapor at 92°C. was determined by Matheson and Moass[14] with another modified version of the Victor Meyer method. The vapor density of formic acid was measured over the temperature range from 10° to 156°C. by Coolidge[15]; and in another modified apparatus, Giguere and Rudle[16] determined the vapor density of hydrazine from 90° to 131°C. Microdetermination methods of the Victor Meyer-type were developed by Peak and Robinson[17], and by Niederl[18], for use at elevated temperatures. By using a porcelain bulb, Meyer and Mensching[19] were able to carry out determinations at temperatures up to 1500°C. Nernst[20] used a 3-ml. iridium bulb for determinations at 2000° C. H. von Wortenberg[21] found that coating the inside and outside of the iridium bulb with magnesium oxychloride decreased the diffusion of the gas through the walls at these high temperatures.

Recently radioactive tracers have been employed in methods for measuring the variation of vapor density with temperature to determine vapor pressures. Dainton and Kimberley[22] determined the variation of vapor pressure with temperature of white phosphorus from -20° to 40°C. by using phosphorus-32 as a tracer, and determining the amount of material in a given volume by beta counting. Barthel and Dode[23] used a similar technique for a study of the partial pressure of bromine above the carbon tetrachloride-bromine system at 0°C. Bromine-82 was used as the radioactive tracer.

None of the methods studied could be easily modified for use with tellurium and polonium over the range of temperatures and pressures of interest. Because of the high specific activity of polonium and the small quantities of material involved, a micromethod capable of several determinations at different pressures and temperatures on the same sample was needed. An original method based on gamma counting of vapor in a standard volume, which was developed and used in this study, is described below.

A known weight of the element, labeled with a gamma emitting radio-isotope, was sealed in a quartz tube of known volume. The tube was heated in a differential temperature furnace so that the two ends of the tube could be maintained at different temperatures. Thus, the vapor at the high-temperature end of the tube was in equilibrium with the condensed phase which collected at the low-temperature end. The activity of the vapor and, therefore, the amount of material present in the vapor, was determined by scintillation counting. Thus, changes in vapor density with temperature at constant pressure were studied by maintaining the temperature of the condensed phase constant and varying the temperature of the vapor. Such measurements could be made over wide ranges of vapor temperatures and pressures.

Effect of Dissociation

Provided only one type of species is present in the vapor, the density of the vapor should vary as predicted by the ideal gas law,

$$PV = \frac{g}{M} RT_A, \qquad (I-1)$$

where

P = pressure

V = volume

R = gas constant

T_A = temperature of the vapor in degrees Kelvin

g = grams of material in vapor

M = molecular weight of vapor.

Substituting vapor density, θ, for g/V and rearranging,

$$\theta T_A = \frac{PM}{R} \quad . \tag{I-2}$$

If the pressure of the system is kept constant, then

$$(\theta T_A)_p = M \times \text{constant}. \tag{I-3}$$

Thus, for measurements made at constant pressure, the product of the vapor density and vapor temperature, (θT_A), will be constant if only one type of species is present in the vapor at the different temperatures.

If dissociation does occur in the vapor, the molecular weight, M, of the vapor will be a weighted average of the molecular weights of the various species present in the vapor, as a result of the dissociation reaction. Because the degree of dissociation will tend to increase with increasing temperatures, the value of M should decrease; and from equation (I-3), $(\theta T_A)_p$ should also decrease.

Thermodynamic Quantities

The following expression is obtained from the Clausius-Clapeyron equation,[24]

$$\log P = \frac{-\Delta H_v}{2.303R} \frac{1}{T_B} + \text{constant}, \tag{I-4}$$

where

ΔH_v = molar heat of vaporization, cals. / mole

P = vapor pressure of liquid, mm.

T_B = temperature of liquid, deg. Kelvin.

Substituting for P, from equation (I-2),

$$\log \left(\frac{\theta T_A R}{M} \right) = \frac{-\Delta H_v}{2.303R} \frac{1}{T_B} + \text{constant}, \qquad \text{(I-5)}$$

or

$$\log \left(\theta T_A\right) + \log \frac{R}{M} = \frac{-\Delta H_v}{2.303R} \frac{1}{T_B} + \text{constant} \qquad \text{(I-6)}$$

For the condition of no dissociation in the vapor, the molecular weight, M, is constant, and equation (I-6) simplifies to

$$\log \left(\theta T_A\right) = \frac{-\Delta H_v}{2.303R} \frac{1}{T_B} + \text{constant} \qquad \text{(I-7)}$$

Thus, a plot of $\log (\theta T_A)$ versus $1 / T_B$ should yield a straight line whose slope is equal to the molar heat of vaporization divided by -2.303R. The molar heat of vaporization, ΔH_v, can therefore be determined directly from vapor density data.

Provided the molecular species is known and remains constant over a given temperature range, the variation of vapor pressure with temperature can be calculated from measurements of vapor density as a function of temperature over this temperature range.

PART II

Experimental

Description of Apparatus

A schematic drawing of the quartz cell, metal housing, differential-temperature furnace, and scintillation gamma counters with the cooling shields and lead bricks in position is shown in Figure 1. The actual assembly used is illustrated in Figure 2. One of the lead bricks has been removed in this Figure to show the position of one of the photomultiplier counters in its cooling shield.

The quartz cells, one of which is illustrated in Figure 3, were made from 9-mm. quartz tubing sealed in a quartz bulb, 25 mm. in diameter, and approximately 37 mm. long. The volume of the cells varied from 11.4 to 15.9 cc.

The metal housing, shown in Figures 1 and 3, was made in three sections from 1.5-in. copper rod and 1.5-in. stainless steel rod. Copper was used for the two end sections; the center section was made of stainless steel. The assembly was machined to house the quartz cell as shown in Figure 1. A copper plug was fitted over the open end of the copper section which contained the bulb-end of cell. Six thermocouple holes were drilled in the two copper sections as shown in Figure 1 to permit introduction of the six platinum-10% rhodium thermocouples. The copper pieces were all plated with 0.010-in. coating of nickel to protect the copper from oxidation

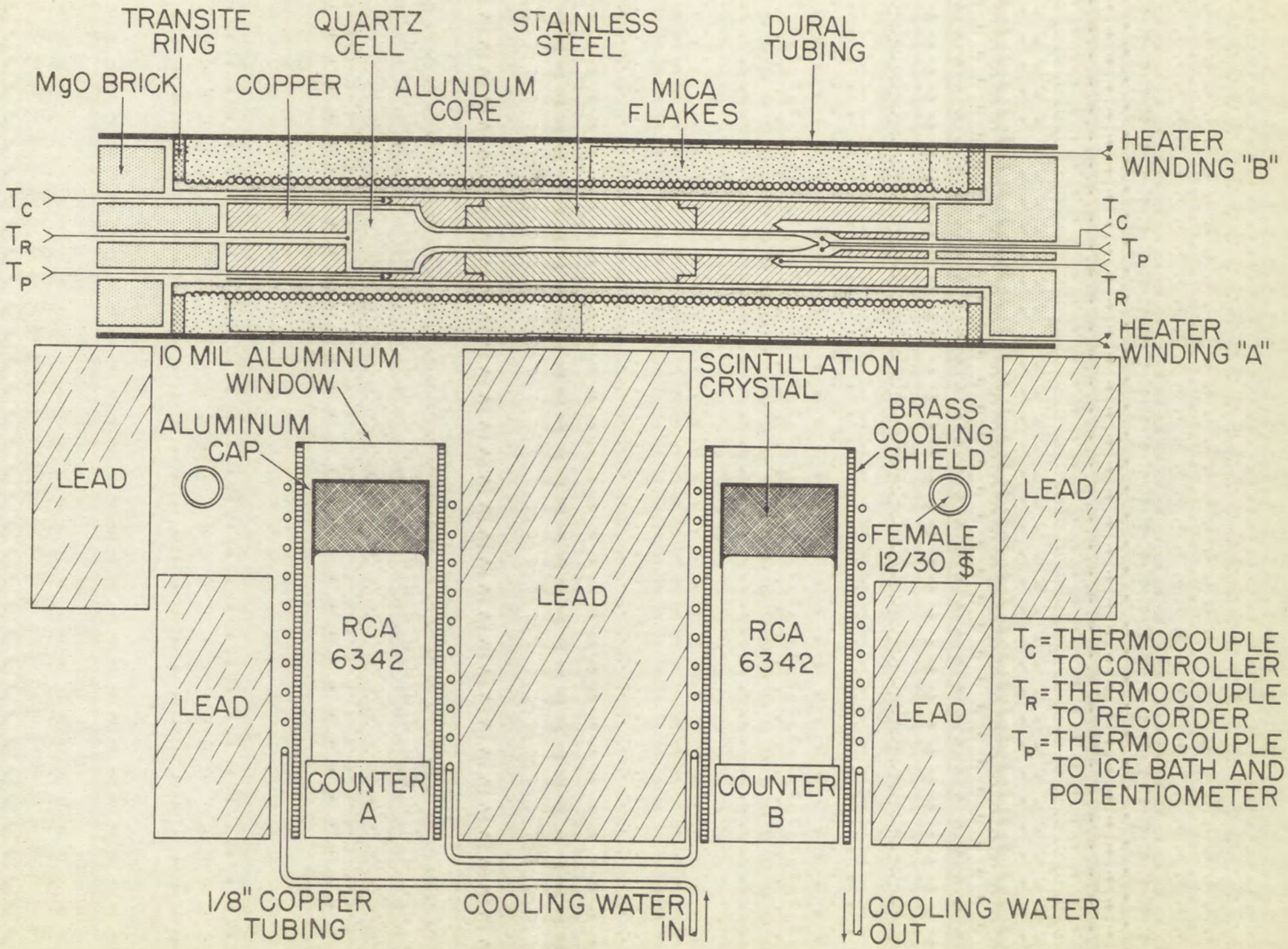

Figure 1. Diagram of Differential Temperature Furnace and Counters Assembly.

Figure 2. Differential Temperature Furnace and Counters Assembly.

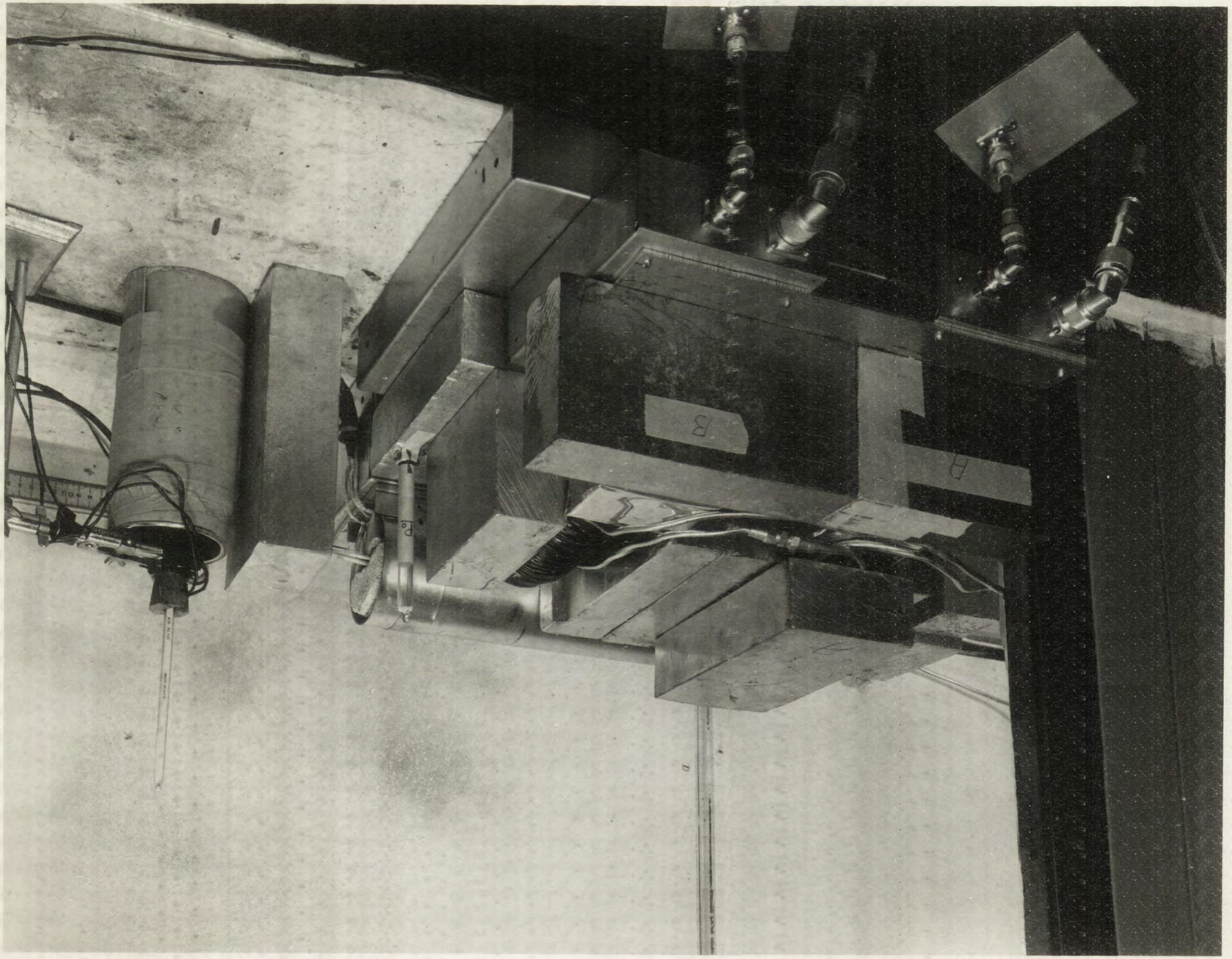

Figure 3. Quartz Cell and Metal Housing

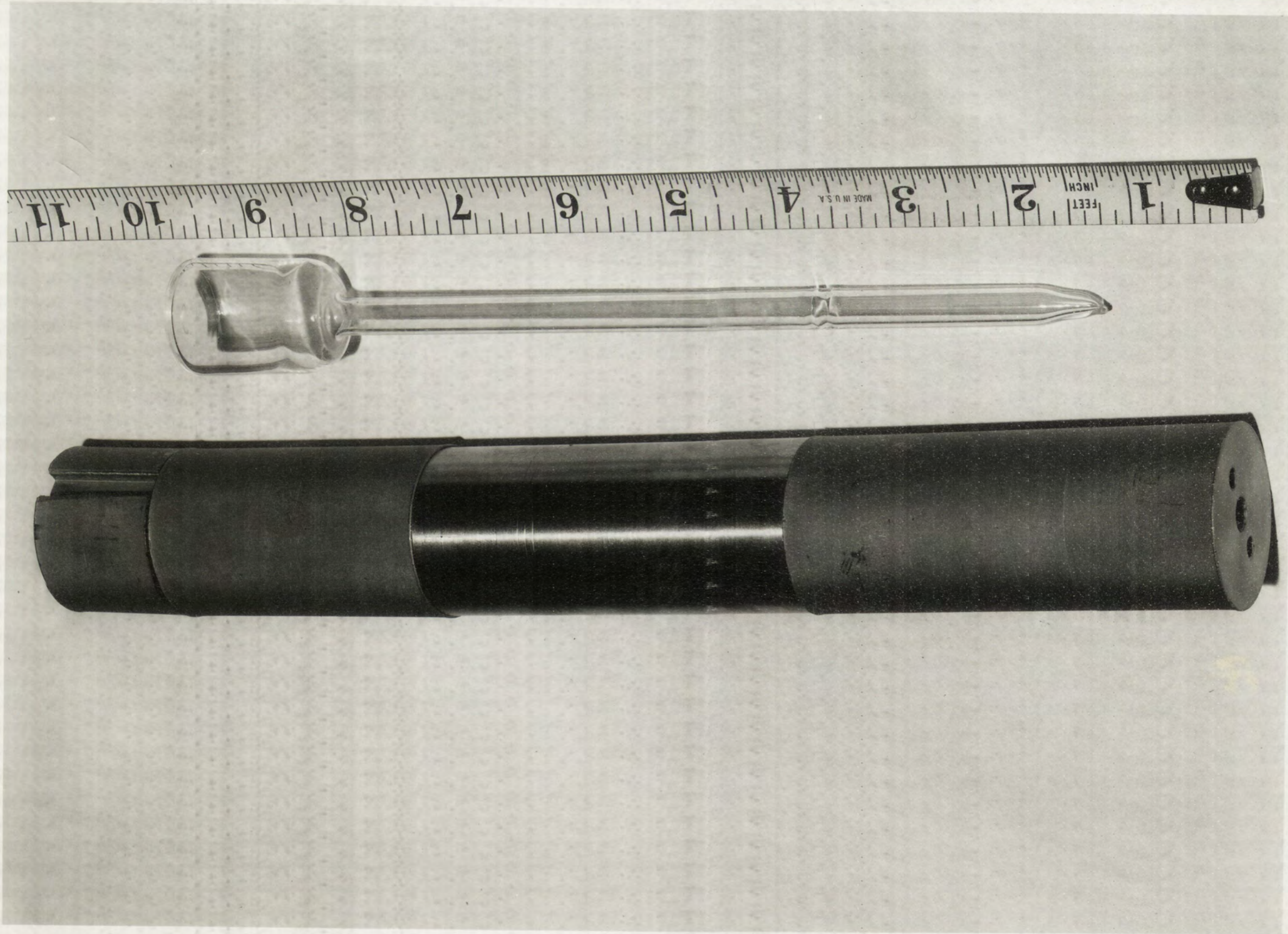
1
2
3
4
5
6
7
8
9
10
11
FEET
INCH
MADE IN U.S.A.

at the elevated temperatures. When it was assembled, the over-all length of the metal housing was 11.5 in.; the outside diameter was machined to 1.44 in.

The differential-temperature furnace is shown in Figures 1 and 2. Two separate heater windings of No. 20 nichrome wire on a 14-in. length of 1.5-in. internal diameter alundum tubing formed the core of the furnace. The alundum tube was centered in a 16.5-in. length of 3.5-in. diameter dural tube by two transite rings. Powdered mica was introduced between the heater windings and the dural tube as insulation. Magnesia plugs fashioned from magnesia bricks were fitted in each end of the furnace. Power to each of the heater windings was individually controlled. This type of control permitted the copper sections to be maintained at constant but different temperatures. The thermal gradient between the two copper sections existed in the stainless steel section.

Temperature Measurement and Control

A schematic drawing of the heater and thermocouple circuits is shown in Figure 4. The position of the thermocouples with relation to the quartz cell is given in Figure 1. Thermocouples, T_c, were used to control the temperatures of the two copper sections. These thermocouples were connected to Model 221 Wheelco controllers adapted with Model 660 Wheelco Capaciline regulators. The units maintained the temperatures of the copper sections constant within 0.2° C. for operating temperatures as high as 1000° C. Thermocouples, T_r, were connected to a two-point Brown Electronik recorder. They served as a

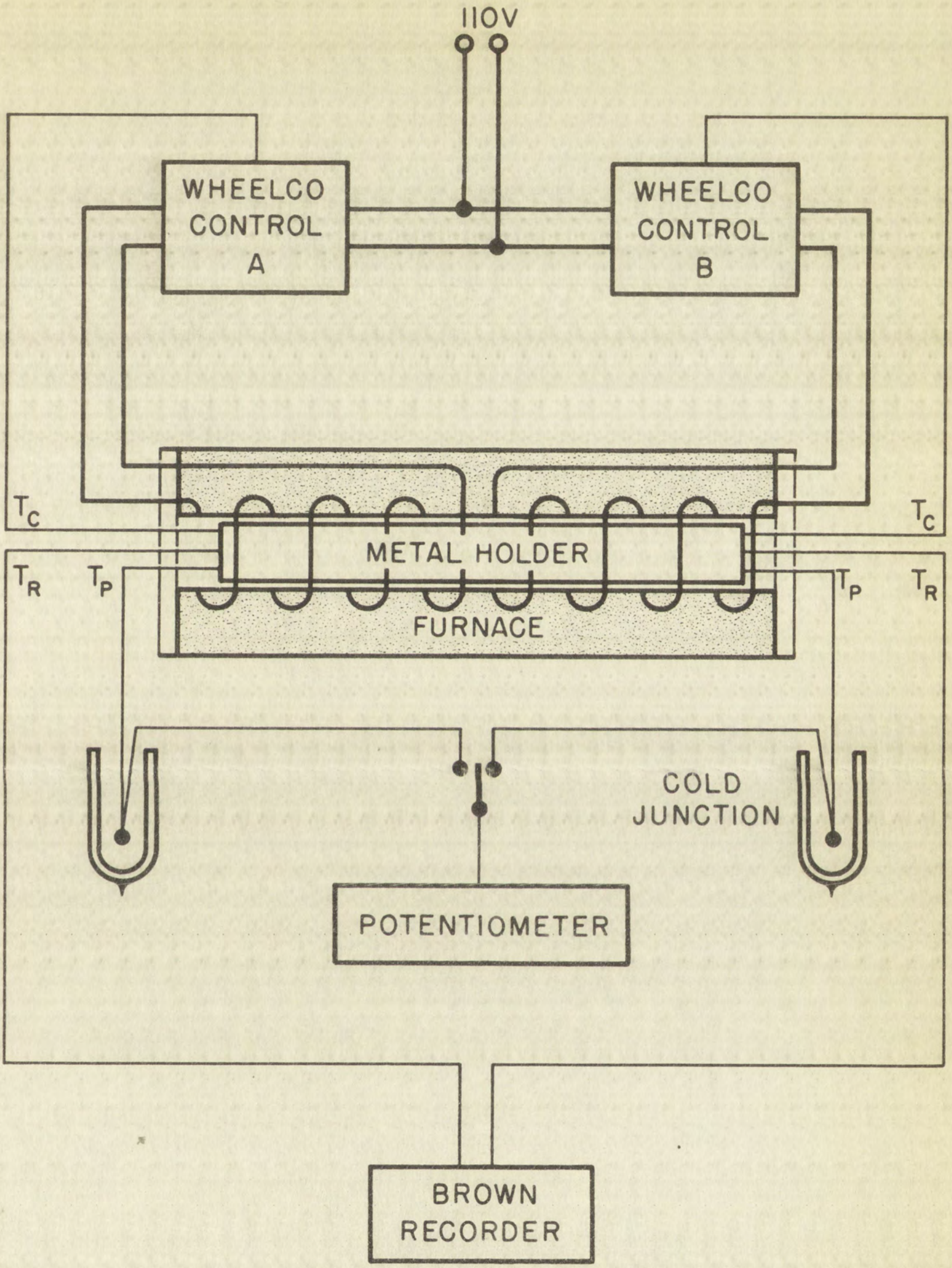

Figure 4. Heater and Thermocouple Circuits.

monitor of the temperature stability of the two copper sections and also indicated when thermal equilibrium was attained for each new temperature setting. Accurate temperature readings were taken with thermocouples, T_p. These thermocouples were connected to an ice-water reference cold-junction; and their potential was measured to the nearest microvolt with a Rubicon K-2 potentiometer.

Description of Method

A sample of the element, labeled with a radioactive isotope, in the case of selenium and tellurium, was distilled under vacuum into the quartz cell. The cell was evacuated to 5×10^{-6} mm. pressure, sealed off, inserted in the metal housing, and the metal housing positioned in the center of the furnace. The six thermocouples were then introduced into the copper sections and the furnace was heated. The temperature of the copper section containing the tube end, B, of the quartz cell was controlled at some fixed temperature, T_B. The temperature of the copper section with the bulb end, A, was controlled at a higher temperature, T_A. The condensed material collected at end B, which was the low-temperature part of the quartz cell. Thus, all of the activity present in the bulb was due to material in the vapor state. The pressure of the vapor in the cell was determined by the temperature, T_B, of the condensed phase. Changes in T_A had no effect on the pressure of the system. By placing lead bricks as shown in Figures 1 and 2, scintillation counter A "saw" only the gamma radiation from the material in the bulb-end of the cell. Counter A was shielded from the radiation emitted by the material at end B. Similarly,

counter B "saw" only the gamma radiation from material at end B of the quartz cell. The counting rates of these two gamma counters therefore indicated where the material was and in what quantity. Determinations of the vapor density were made at various temperatures of T_A and T_B. The temperature T_B was raised until further increase no longer resulted in an increased counting rate at A. At this point, all of the material in the cell was vaporized. The temperatures of the two ends were equalized and the counting rate at A determined. Because this value of counting rate corresponded to the vapor density when all of the material occupied the volume of the cell as vapor, it served as a factor for converting counting rates to density for all the counts taken. Measurements were then taken as the temperatures T_A and T_B were decreased. This procedure of taking measurements both as the temperatures were increased and as they were decreased served as a check as to whether the system was at equilibrium for each of the determinations. Variations of vapor density with temperature at constant pressure were determined by keeping T_B constant and varying T_A. Changes in vapor density as a function of the pressure were determined by varying T_B and keeping T_A at a slightly higher temperature relative to T_B.

Effect of Decay

The amount of radioactivity in the samples changed continually due to radioactive decay. A counting standard was prepared for each of the elements studied in order to eliminate the need of correcting for decay and to provide a correction for changes in counter response. Since individual runs on the samples took several days, the counting standards

proved to be a necessity.

Effect of Decay Products

The tellurium activity consisted of tellurium-121 and tellurium-123 which decay by internal transitions. Thus, no decay products were formed. For selenium, the isotope selenium-75 was used. This decayed to inactive arsenic-75. However, because the total amount of arsenic formed by decay was less than 0.0001% of the selenium, any depression of the vapor pressure of selenium due to possible solution of the arsenic would be so small that it could be ignored.

With the polonium the effect of decay products was of considerable importance. Since the material was a single isotope, polonium-210, of high specific activity, the formation of helium and lead by radioactive decay was appreciable. The lead daughter grew in at the rate of 0.5 atomic per cent per day. Beamer and Maxwell[25] in their studies of the structure of polonium metal found that the lead impurity was miscible with the polonium to at least 50 atomic per cent. Witteman, Giorgi, and Vier[26] found that lead forms an intermetallic compound with polonium. Thus, it appeared that lead was an undesirable impurity. To minimize the effect of this unavoidable impurity, it was necessary to make determinations as soon after the purification step as possible. Measurements were taken over a two-day period on freshly purified material. One sample of polonium was studied over an extended period of time to determine the effect of the decay products.

Preparation of Chemical Reagents

Polonium

Polonium-210 was used in this study. It is an alpha emitter with a

138.4-day half-life and decays to stable lead-206. Although the isotope is essentially a pure alpha emitter, it also emits 0.047-Mev gammas at the rate of 3.7×10^5 gammas per curie second. Polonium is produced artificially by the thermal-neutron irradiation of bismuth metal,

$$_{83}Bi^{209} + {}_{0}n^{1} \dashrightarrow {}_{83}Bi^{210} + \gamma \qquad \text{(II-1)}$$

and the subsequent decay of the bismuth-210 by beta emission,

$$_{83}Bi^{210} \dashrightarrow {}_{84}Po^{210} + \beta^{-} \qquad \text{(II-2)}$$

Ten curies (2.225×10^{-3} gms.) of polonium were obtained through the Los Alamos Scientific Laboratory. The polonium was received as a metallic deposit on tantalum gauze, contained in a capped tantalum crucible, sealed in an evacuated glass capsule. Since the material contained lead-206 from decay, as well as other minor impurities, it was purified before each run. For the purification, the vacuum distillation technique of R. Krohn[27] and the electrodeposition method described by Bowman and Krikorian[28] were used. All operations were conducted in hooded areas with strong air flows. Rubber gloves were used to protect the hands from contamination, and special glassware was constructed for the various manipulations. All of the operations involving polonium solutions were carried out in the lucite box, Figure 9. These elaborate dissolution and plating methods were necessary, since even a few minute droplets of polonium solution would cause serious contamination of the hood and surrounding areas.

The purification process was carried out in four stages:

Stage 1 - Distillation of polonium from tantalum gauze onto a

clean glass surface.

(a) The glass capsule was opened by the file-mark and thermal-shock technique. The cap was removed from the tantalum crucible (1 cm. x 5 cm.) containing the gauze and the crucible inserted in the special glass distillation apparatus shown in Figure 5.

(b) The distillation unit was assembled and connected to the vacuum system, Figure 6.

(c) The oscillator coil from a 100-watt induction heater, constructed from the circuit diagram of Rupert[29], was positioned around the distillation unit. The coil was adjusted so that the tantalum crucible was centered in it, Figures 5 and 7.

(d) The unit was evacuated to a pressure of 5×10^{-6} mm. and the tantalum "gun" heated to a dull red heat by induction. A silvery mirror of polonium metal deposited on the glass surface of the upper section of the apparatus.

(e) After three minutes heating time, the induction heater was turned off and the system allowed to cool.

Stage 2 - Dissolution of the polonium mirror.

(a) Helium gas was introduced into the cooled system and the apparatus was separated at the 45/50 $\frac{T}{S}$ joint.

(b) The upper section, 2 in Figure 8, containing the polonium mirror on surface A was inverted and a second glass section, 1 in Figure 8, was fitted to it for the dissolution of polonium.

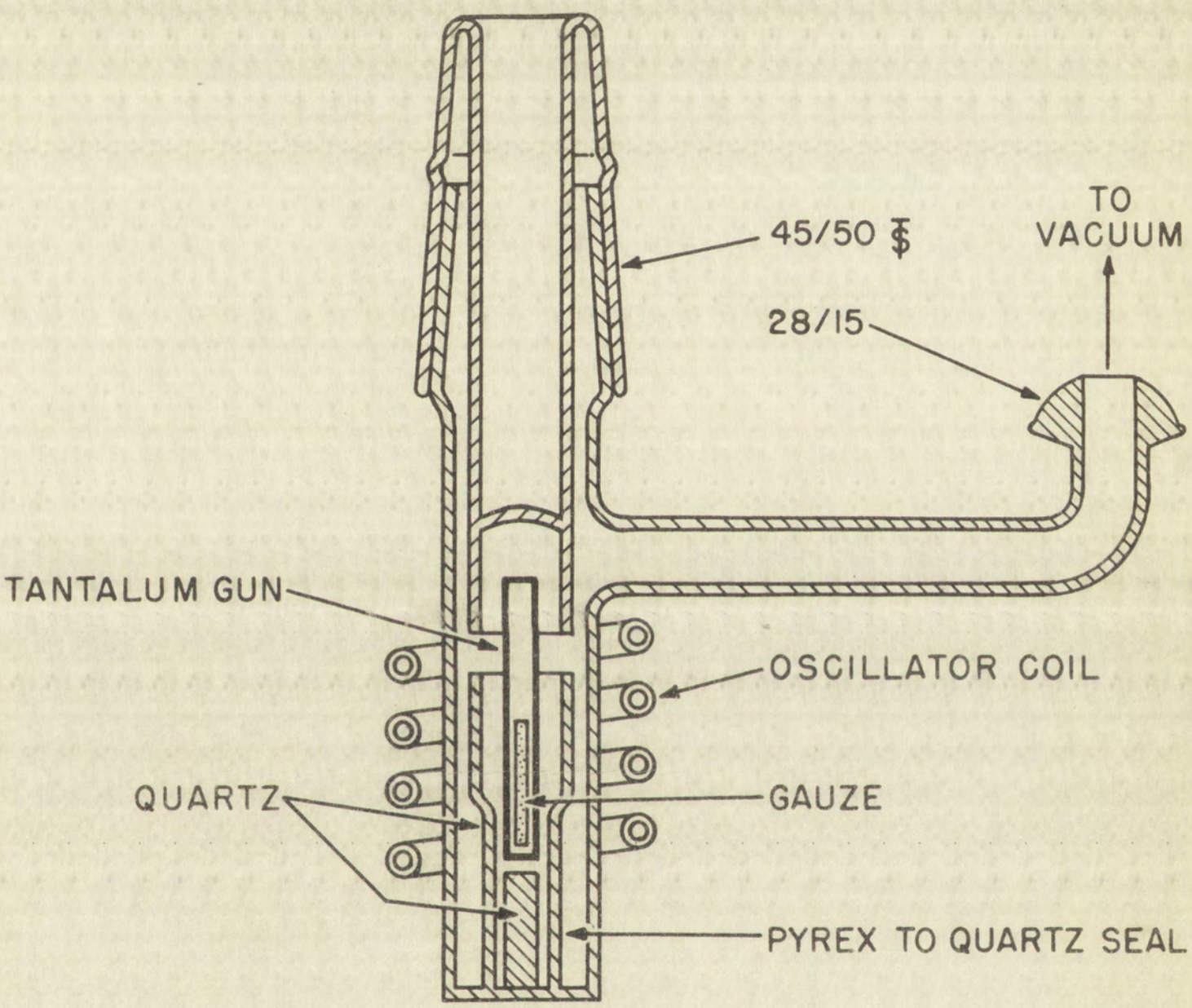

Figure 5. Distillation Apparatus

Figure 6. Vacuum Line with Distillation Apparatus.

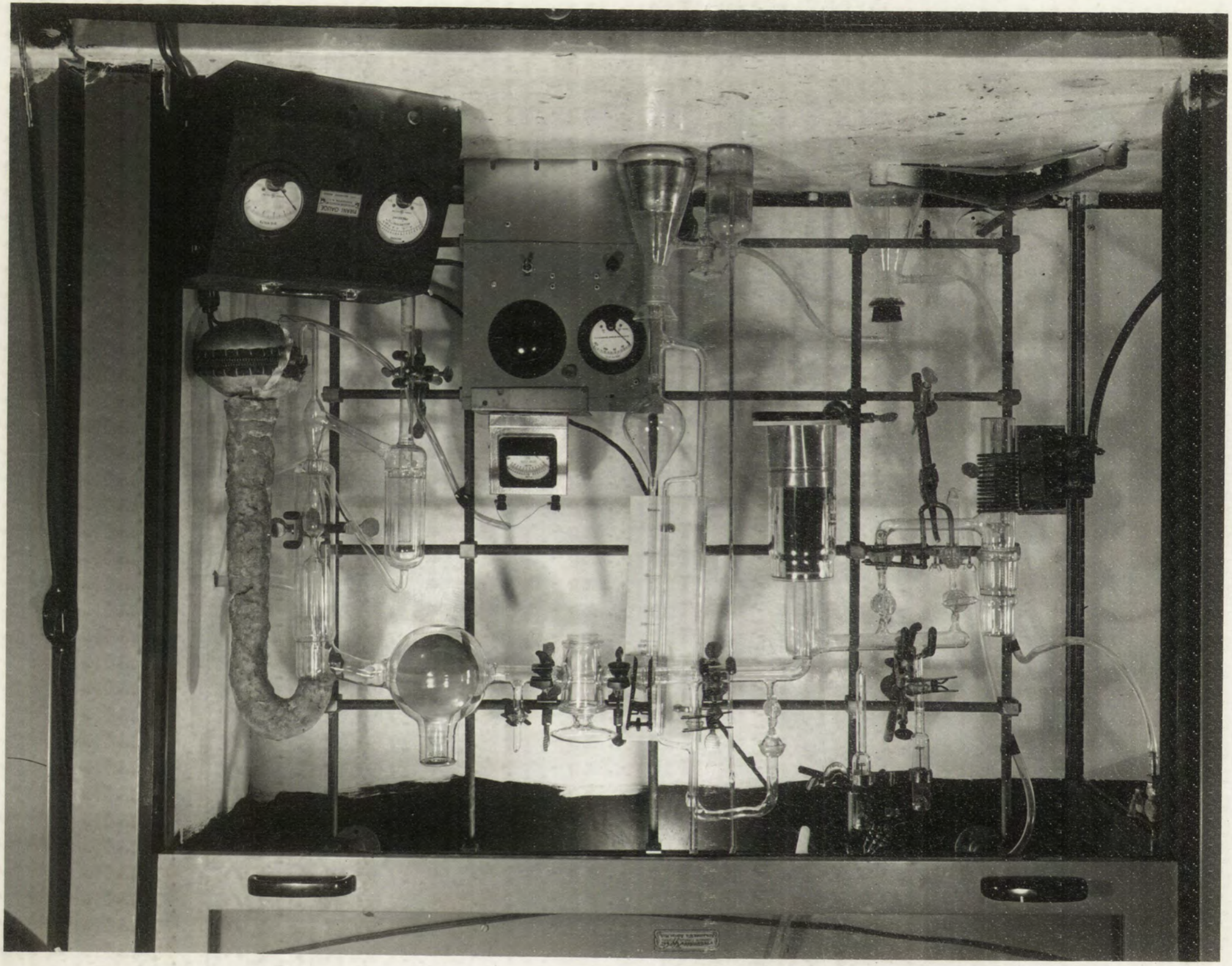

Figure 7. Distillation Apparatus and Oscillator Coil.

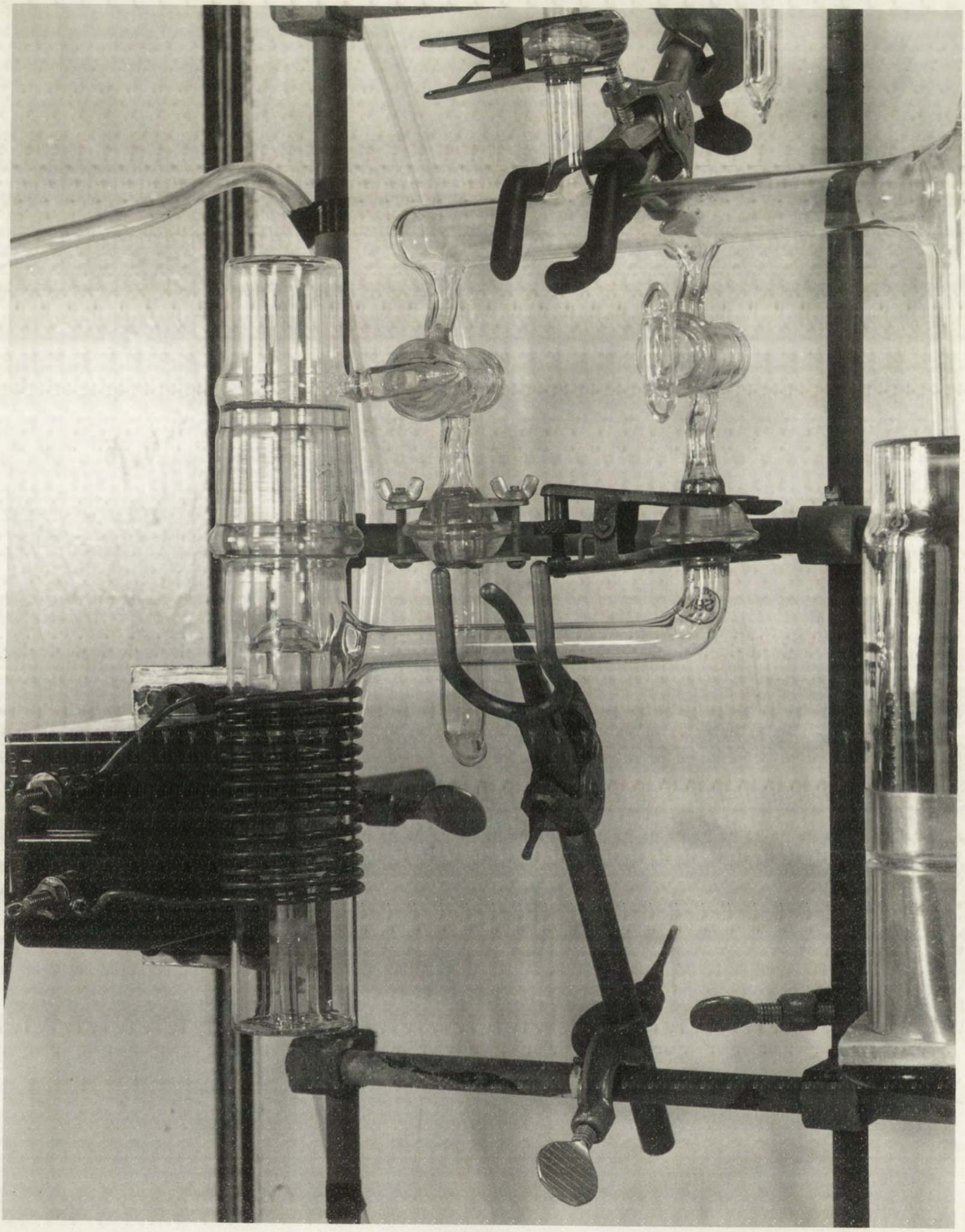

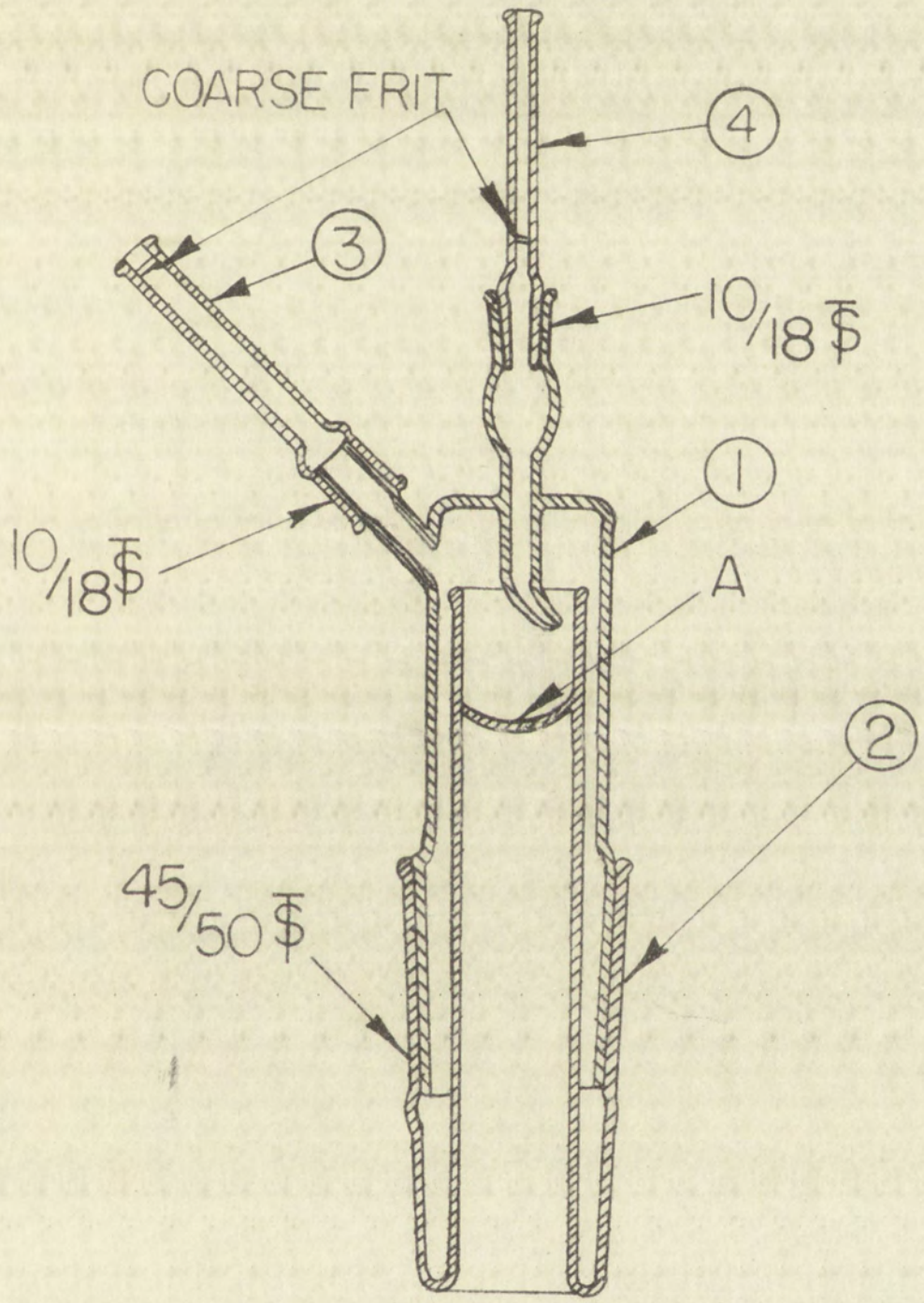

Figure 8. Dissolution Apparatus for Polonium.

(c) The polonium was dissolved by addition of 10 ml. of 7.8 M nitric acid through tube 4, Figure 8, while applying gentle suction through tube 3.

(d) The unit was carefully separated at the 45/50 T_S joint and the acid solution poured into the plating beaker, Figures 9 and 10. A 250-ml. beaker with a side arm attached was used as the plating cell.

(e) Using the same procedure, additional 10-ml. portions of nitric acid solution were used to rinse out surface A until a total of 40 ml. of acid had been added.

(f) The unit was then thoroughly rinsed with distilled water, and the washings added to the beaker.

Stage 3 - Electrodeposition of polonium from nitric acid solution onto a tantalum gauze.

(a) The volume of the solution in the plating beaker was adjusted to 200 ml. with distilled water, to make the final acid concentration 1.5 M.

(b) A platinum foil, 7 cm. x 13 cm., was used as the anode, and a 1 cm. x 4 cm.-section of surgical tantalum gauze was the cathode.

(c) The electrodeposition was conducted at a constant cathode potential of 0.3 volts in order to obtain good separation from dissolved impurities.[30] The cathode potential was maintained at a constant value with respect to a Beckman, Model 270, saturated calomel electrode, through the use of an automatic plating control.[31]

Figure 9. Polonium Electrodeposition Set-up in Lucite Box.

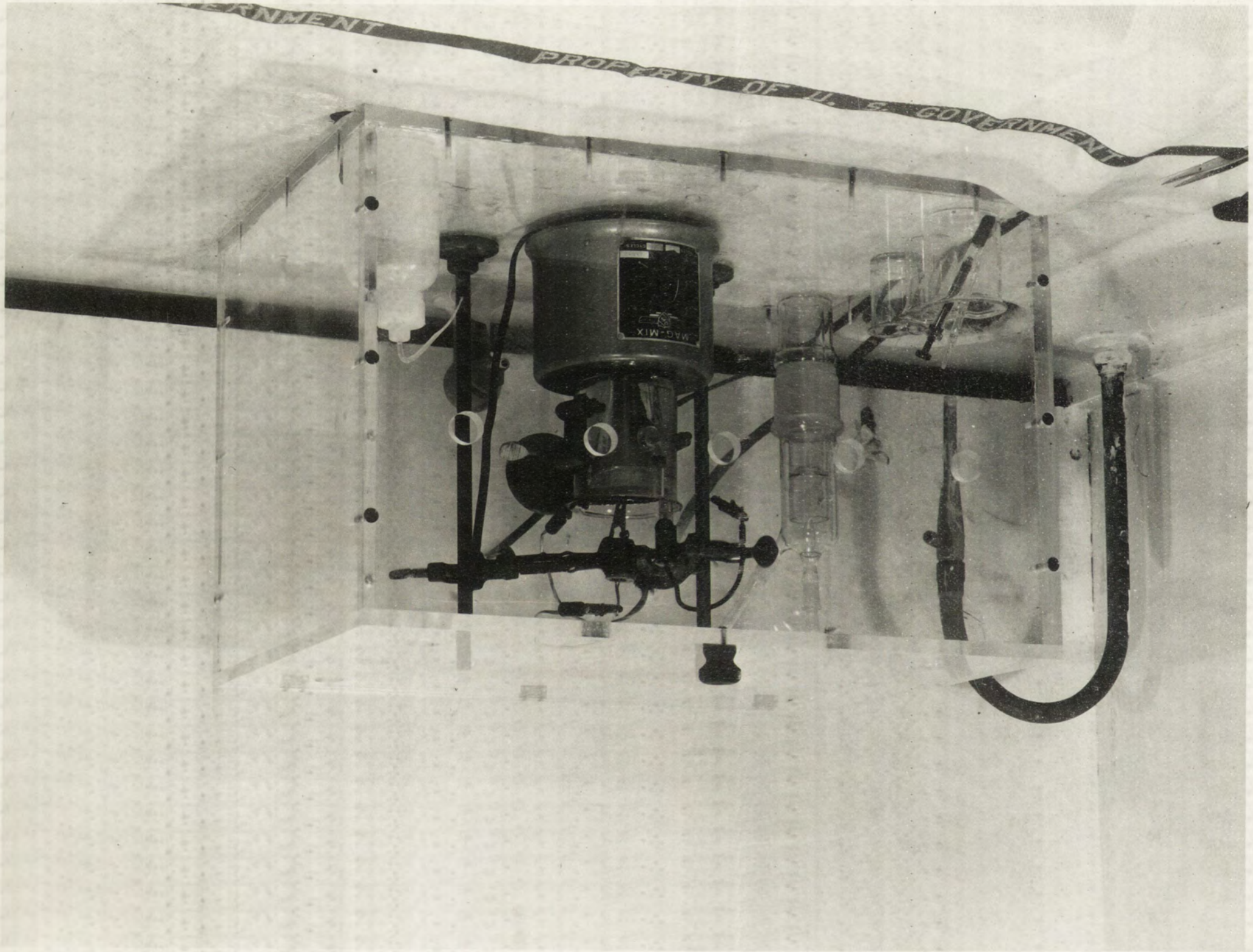
PROPERTY OF U. S. GOVERNMENT
MAG-MIX

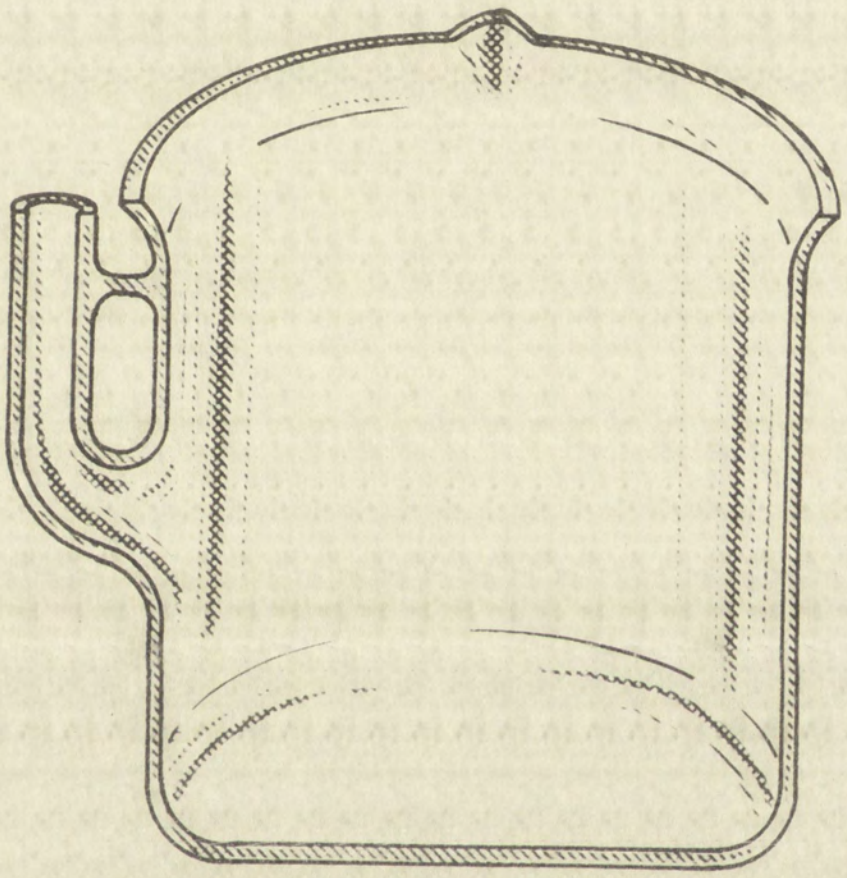

Figure 10. Polonium Plating Cell.

This plating control maintained the potential difference between the cathode and the reference calomel electrode at a constant preset value by automatically varying the potential across the anode and cathode of the plating cell. The circuit diagram of the plating control used is given in Figure 11.

(d) The solution in the plating cell was stirred by rotation of a small, glass-encased, permanent magnet in the beaker. The rotation was brought about by placing the beaker with magnet on a magnetic stirring apparatus (Mag-Mix Figure 9).

(e) The polonium content of the plating solution was followed by assay of the alpha activity of aliquots of the stirred solution. Micro-pipettes of 0.010 ml. capacity were used for sampling. The aliquot, together with the micro-pipette washings, was delivered onto a 2-cm. diameter tantalum disk and evaporated to dryness with an infrared bulb. The alpha activity was then determined by counting in a low-geometry methane-flow alpha counter.

Stage 4 - Distillation of polonium into the quartz cell.

(a) When the desired amount of polonium had been deposited on the tantalum cathode, the gauze was removed from the plating cell.

(b) The tantalum gauze was washed with distilled water, then with acetone and allowed to dry. Because the alpha decay of polonium generated considerable heat, drying of the acetone occurred very quickly.

(c) The tantalum gauze with the polonium deposit was placed in the quartz cell apparatus for final distillation into the quartz cell.

Figure 11. Schematic Drawing of Automatic Plating Current Control.

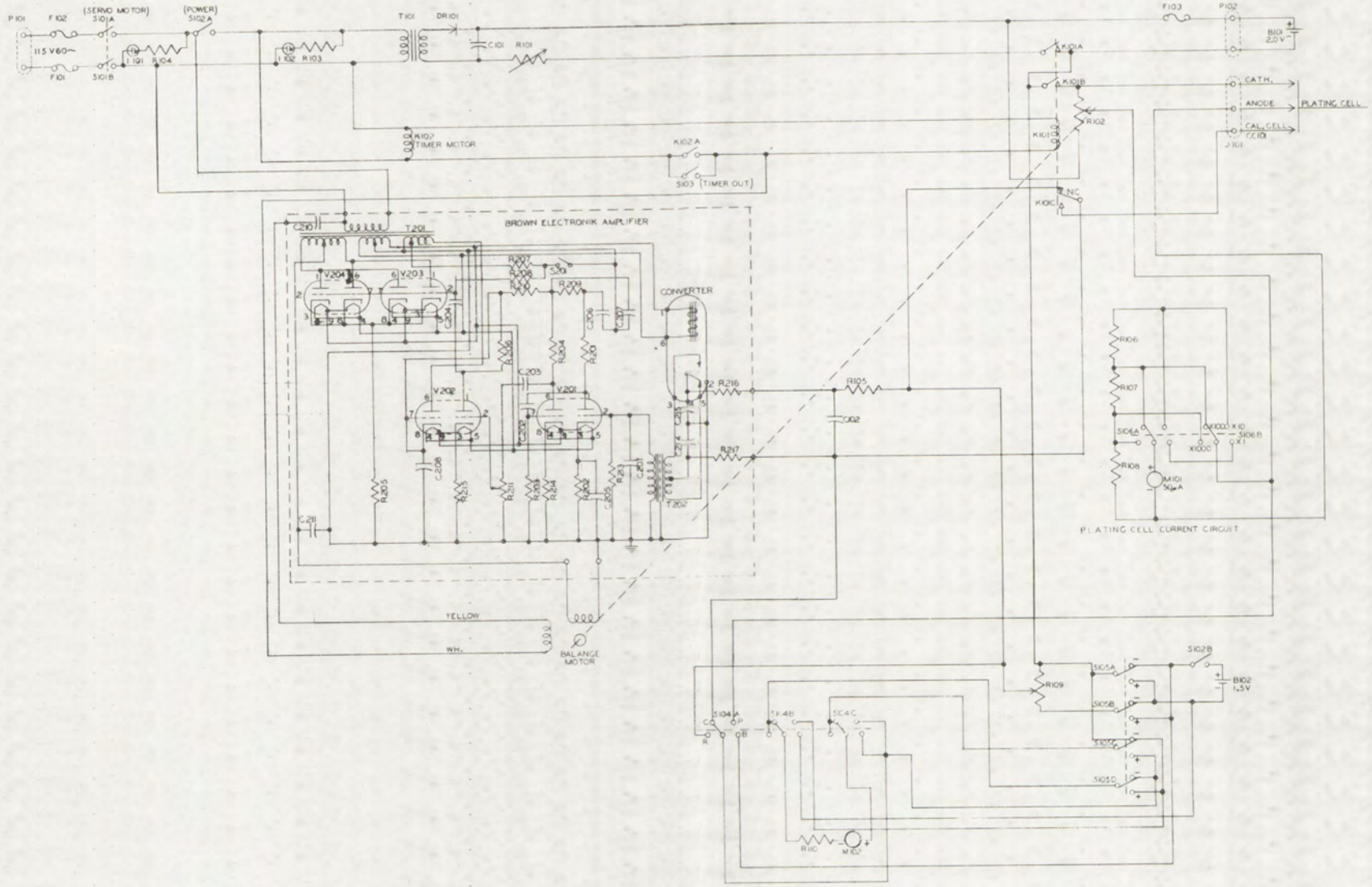

BILL OF MATERIAL			
PART NUMBER	NUMBER REQ.	FOR	DESCRIPTION
B101	1		WILLARD DA-2-1 2 VOLT
B102	1		BURGESS 4FH OR EQUIV.
C101	1		40 MF 250V C-D UP4025
C102	1		TYPE W P 400 MF, 6V NP
DR101	1		½ FEDERAL 179033
F101	1		3AG 2A
F102	1		3AG 2A
F103	1		3AG 2A
I 01	1		NE 51
I 02	1		NE 51
J 01	1		TYPE AN 3100 14S-1
K 01	1		4PDT ALLIED CONTROL
K 02	1		SPST LUMENITE MODEL E III
M 01	1		WESTON 301 50 MICROAMP
M 102	1		AS 101 WITH 3 VOLT SCALE
P101	1		AMPHENOL 61 M10
P102	1		JONES P 302 AB
R 01	1		MALLORY 2AV 2000
R102	1		25 OHM HELIPOT TYPE A
R 103	1		180K IN SOCKET
R 104	1		SAME AS 103
R 105	1		4500 OHM ½ W A-B
R 106	1		500 MICROAMPERE SHUNT
R 107	1		5 MILLIAMPERE "
R 108	1		50 MILLIAMPERE "
R 109	1		1000 OHM HELIPOT TYPE A
R 110	2		30K IRC WW3 IN SERIES
S101	1		DPDT ARROW H-H 1333
S102	1		SAME AS 101
S103	1		SPST ARROW H-H 1330
S104	1		3P4T MALLORY 3234 J
S105	1		4P2T CENTRALAB 1409
S106	1		3P4T MALLORY 3234 J
T101	1		THORDARSON T 23V25
C201	1		.015 MF.
C202	1		.05 MF
C203	1		.05 MF
C204	1		.05 MF
C205	1		.25 MF
C206	1		10 MF
C207	1		10 MF
C208	1		10 MF
C210	1		1 MF
C211	1		1 MF
C214	1		.25 MF
C215	1		.25 MF
R201	1		1 MEG.
R202	1		10 K
R203	1		1 MEG.
R204	1		1 MEG.
R205	1		150
R206	1		1 MEG.
R207	1		10 K
R208	1		150K
R209	1		150K
R210	1		47K
R211	1		1 MEG.
R213	1		100K
R216	1		300
R217	1		300
S201	1		SPST
T201	1		POWER TRANSFORMER
T202	1		INPUT TRANSFORMER
V201	1		12AX7
V202	1		12AX7
V203	1		12AU7
V204	1		12AU7
R214	1		1800
R215	1		1800
C0101	1		CALOMEL CELL BECKMAN 270

Tellurium

A mixture of 150-day tellurium-121 and 121-day tellurium-123 was used as the radioactive tracer for tellurium. The activity was artificially prepared by the deuteron-bombardment of an antimony target[32] in the Los Alamos cyclotron, and resulted from the nuclear reactions,

$$_{51}Sb^{121} + {}_{1}H^{2} \dashrightarrow {}_{52}Te^{121} + 2\,{}_{o}n^{1} \qquad \text{(II-3)}$$

$$_{51}Sb^{123} + {}_{1}H^{2} \dashrightarrow {}_{52}Te^{123} + 2\,{}_{o}n^{1} \qquad \text{(II-4)}$$

The antimony target was prepared by electrodeposition of a 0.005-in. coating of antimony on a copper base from an antimony acid-fluoride plating bath.[33] The target was irradiated for 2 hours with a deuteron beam of 25 microamperes.

The tellurium activity was recovered from the antimony and purified for use in the quartz cell by the following procedure which was carried out in five stages:

Stage 1 - The removal of the antimony coating from the copper base.

(a) The antimony coating was scrapped off the copper base with a steel spatula. The copper base was held under water during the scrapping operation to prevent loss of material.

Stage 2 - Separation of tellurium activity from the antimony and copper.

(a) The antimony was collected on a fritted-glass

filtering crucible.

(b) The antimony was dissolved in 30 ml. of 4 N nitric acid and the resulting solution filtered.

(c) The acid filtrate was slowly evaporated almost to dryness.

(d) The hot residue was dissolved in 10 ml. of concentrated hydrochloric acid.

(e) One-half milliliter of tellurium carrier (0.020 g./ ml. of tellurium in 3 N hydrochloric acid) was added.

(f) The solution was slowly evaporated almost to dryness to remove the nitric acid.

(g) The residue was dissolved in 20 ml. of 3 N hydrochloric acid and the resulting solution was heated on a water bath.

(h) The tellurium in the solution was then reduced to the metal by addition of 5 ml. of 3 N hydrochloric acid, saturated with sulfur dioxide, followed by 2 ml. of 15% hydrazine-hydrochloride solution.

(i) The slurry was heated on a water bath for 8 minutes and the tellurium precipitate recovered by filtration. The filtrate, containing the antimony, copper, and other soluble impurities, was discarded.

(j) The tellurium precipitate was washed with 10 ml. of 3 N hydrochloric acid, saturated with sulfur dioxide.

(k) The tellurium precipitate was then washed with two 10-ml. portions of hot water.

Stage 3 - Dissolution of tellurium metal.

(a) The tellurium metal was dissolved in 2 ml. of concentrated nitric acid and the resulting solution was filtered.

(b) The filter was washed with 5 ml. of hot nitric acid followed by 10 ml. of water, and the filtrate and washings were transferred to an erlenmeyer flask.

(c) The solution was slowly evaporated to about 1 ml., to remove the nitric acid.

(d) The residue was dissolved in 10 ml. of concentrated hydrochloric acid and the solution was slowly evaporated to about 1 ml.

(e) Step (d) was repeated.

(f) The residue was dissolved in 10 ml. of 3 N hydrochloric acid and the solution was filtered. This acid solution was divided into two portions. One portion was used in the preparation of the counting standard and the other for the preparation of the tellurium sample.

Stage 4 - Reprecipitation of the tellurium metal.[34]

The two portions of the tellurium solution were treated separately to effect reduction to tellurium metal by the following procedure:

(a) The tellurium solutions were heated on a water bath

and the tellurium metal precipitated by the addition of 4 ml. of 3 N hydrochloric acid, saturated with sulfur dioxide, and 1 ml. of 15% hydrazine-hydrochloride solution.

(b) The slurries were heated for 8 minutes and the tellurium precipitates recovered by filtration.

(c) The precipitates were washed with 10 ml. of 3 N hydrochloric acid, saturated with sulfur dioxide, followed by nine successive washings with 5-ml. portions of hot water.

(d) The precipitates were then washed with two 5-ml. portions of ethyl alcohol into centrifuge tubes and the precipitates caused to settle out by centrifugation.

(e) The supernatant alcohol was poured off and the precipitates dried at 90° C. for 1 hour.

(f) The precipitates were heated overnight at 120° C. under vacuum.

Stage 5 - Distillation of tellurium into the quartz cell and counting standard assemblies.

One of the precipitates was used for the preparation of the counting standard. The other precipitate was introduced into the quartz-cell assembly for final distillation into the quartz cell.

The above described procedure was repeated using a dummy antimony target on a copper base, and the final tellurium precipitate submitted for spectographic analysis. The analysis showed less than 0.01% antimony present and only traces of other elements.

Selenium

Selenium-75 was used as the radioactive tracer for selenium. This isotope was produced by the deuteron-bombardment of an arsenic target[35] in the Los Alamos cyclotron. The nuclear reaction is,

$$_{33}As^{75} + {}_{1}H^{2} \dashrightarrow {}_{34}Se^{75} + 2\,{}_{o}n^{1} \qquad \text{(II-5)}$$

The arsenic target was prepared by the electrodeposition of a 0.005-in. coating of arsenic on a copper base from an arsenic-hydrochloric acid plating bath.[36] The target was irradiated for 5 hours with a deuteron beam of 25 microamperes.

The selenium activity was recovered from the arsenic and purified for use in the quartz cell by the following procedure which was carried out in six stages:

Stage 1 - Removal of the arsenic coating from the copper base.

(a) The arsenic coating was scrapped off the copper base with a steel spatula. The copper base was held under water during the scrapping operation to prevent loss of material.

Stage 2 - Separation of selenium activity from arsenic and copper.

Because the arsenic scrappings contained an appreciable amount of copper, the selenium activity was collected on a ferric hydroxide precipitate by the method of W. R. Schoeller.[37]

(a) The arsenic was collected on a fritted-glass filtering-

crucible.

(b) The arsenic was dissolved in 30 ml. of warm 1:1 nitric acid and the solution filtered.

(c) The acid solution was slowly evaporated to about 15 ml., and then, transferred to a centrifuge tube.

(d) Two milliliters of ferric nitrate solution (0.0055 g./ml. of iron in dilute nitric acid) was added.

(e) The solution was heated on a water bath and excess ammonium hydroxide was added dropwise to precipitate the ferric hydroxide.

(f) After 10 minutes heating, the slurry was centrifuged and the supernatant liquid containing the copper, arsenic, and other soluble impurities was discarded.

(g) The ferric hydroxide precipitate was washed with 20 ml. of hot water containing ammonium hydroxide and ammonium chloride.

(h) Step (g) was repeated three times.

Stage 3 - Separation of selenium activity from iron.[38]

(a) The ferric hydroxide precipitate was dissolved in 10 ml. of 6 N hydrochloric acid and the solution filtered.

(b) One milliliter of selenium carrier (0.012 g./ml. of selenium in 6 N hydrochloric acid) was added.

(c) The acid solution was heated and freshly prepared 20% stannous chloride, in concentrated hydrochloric acid, was added dropwise until a brown-black precipitate of selenium formed.

(d) The precipitate was collected on a fritted-glass filtering

crucible and washed with 1.0 N hydrochloric acid containing stannous chloride.

(e) The precipitate was then washed three times with 2% hydrochloric acid, and the filtrate containing the iron and other soluble impurities was discarded.

(f) The precipitate was dissolved in a minimum amount of concentrated hydrochloric acid, saturated with bromine, and the solution filtered.

Stage 4 - Reduction of selenium in solution to the metal with sulfurous acid.

(a) The acid-bromine solution was cooled in an ice-bath and sulfur dioxide gas was bubbled into the solution until the bromine color disappeared.

(b) The sulfur dioxide gas was bubbled through the solution for an additional 15 minutes and the resulting selenium precipitate was allowed to settle overnight.

Stage 5 - Dissolution and reprecipitation of selenium.

(a) The selenium precipitate was dissolved by the careful addition of 1 ml. of concentrated nitric acid.

(b) The solution was cooled and 1 ml. of 1:1 sulfuric acid was added.

(c) After cooling, 1 g. of urea was added to destroy the nitric acid.

(d) The acid solution was carefully evaporated almost to dryness.

(e) The residue was dissolved in 10 ml. of 6 N hydrochloric acid and the solution was divided into two portions for use in the preparation of the selenium sample and the counting standard.

(f) The two portions of acid solution were cooled and the selenium precipitated by passing in sulfur dioxide gas, as before.

(g) The selenium precipitates were washed with 6 N hydrochloric acid saturated with sulfur dioxide.

(h) The precipitates were then washed with nine successive 5-ml. portions of hot water and then transferred to centrifuge tubes with two 5-ml. portions of alcohol

(i) The precipitates were finally washed with diethyl ether and dried for 1 hour at 90°C.

(j) The precipitates were heated overnight at 120° C. under vacuum.

Stage 6 - Distillation of the selenium into the quartz-cell and the counting-standard assemblies.

One of the precipitates was used for the preparation of the counting standard. The other precipitate was introduced into the quartz-cell assembly for distillation into the quartz cell.

The above procedure was repeated using a dummy arsenic target on a copper base, and the final selenium precipitate was submitted for spectographic analysis. The analysis showed less than 0.01% arsenic, copper, and iron, and only traces of the other elements.

Analytical Reagents

Standard solutions of sodium thiosulfate, ferrous ammonium sulfate, and potassium dichromate were prepared according to the methods of Hillebrand and Lundell.[39] The sodium thiosulfate solution was standardized against a standard iodine solution.[40] The potassium dichromate solution was prepared by direct weighing of the pure salt.

Freshly prepared starch solution was used as the indicator in the thiosulfate titrations. Diphenylamine was used as an internal indicator for the dichromate-ferrous sulfate titrations.

Preparation of Samples

The quartz cell assembly as originally constructed, consisted of the quartz bulb and tube, shown in Figure 3, attached through a constriction, to a quartz-pyrex graded seal with a 28/15 male ball joint at the open end. The active material was introduced into the ball joint and the assembly connected to the vacuum line. After the system had been evacuated to a pressure of 5×10^{-6} mm., the assembly was flame-sealed off between the ball joint and the graded seal. The active material was positioned at the closed end of the tube and then distilled into the graded-seal area by placing the end of the tube in a tube furnace and heating to 600°C. The graded seal-quartz cell portion of the assembly extended outside the furnace. The pure material formed a mirror on the wall of the glass tube where it protruded from the furnace. The assembly was then inserted further into the furnace so that all of the graded seal area and part of the quartz cell were

heated; the active material distilled into the quartz cell. The unit was allowed to cool, and the quartz cell containing the active material was sealed off at the constriction, to give the quartz-cell unit shown in Figure 3.

For the preparation of the polonium samples, the activity was introduced into the ball joint as a metallic deposit on tantalum gauze. The selenium and tellurium activities were introduced as pellets. The above two-stage distillation procedure was used in the preparation of all samples.

Preparation of Counting Standards

The counting standard assembly was prepared by attaching a 28/15 male ball joint to a 10-in. length of 7-mm. pyrex tubing sealed at one end. The active material was introduced into the ball joint and the assembly evacuated. The unit was then flame-sealed off between the ball joint and the 7-mm. tubing with the active material contained in the section attached to the 7-mm. tubing. The activity was then distilled into the end of the 7-mm. tubing by placing the unit in the tube-furnace as before. A one-inch length of the 7-mm. tubing was finally flame-sealed off. It contained all of the activity. This length of 7-mm. tubing was positioned with sealing wax in the center of the tube of a full-length male 12/30 $\frac{T}{S}$ joint. Two female 12/30 $\frac{T}{S}$ joints had been cemented into holes in two lead bricks used for shielding, Figure 1. Fiducial marks were placed on the outside of the male joint containing the counting

standard and on the female joints cemented in the lead bricks to insure constant counting geometry for every counting-rate determination of the standards. The polonium counting standard in position for counting is shown in Figure 2.

Because the counting standards were used only to compensate for decay of activity and changes in response of the scintillation counters during a run, it was not necessary to know the actual amount of activity present in the standard samples. Instead, only the percentage change in counting rate of the standard at any one time relative to the counting rate of the standard at a specific time was determined. The specific counting rate used, was the counting rate of the standard at the time of complete vaporization of the sample.

Calibration of Volume of Quartz Cells

The volume of each quartz cell was determined by weighing the water required to fill the cell. The cells were first weighed empty on an analytical balance. They were then filled to the seal-off constriction with distilled water and the total weight determined. From the weight of water and its density, the volume of the cell was calculated as follows:

$$\text{Volume of cell} = \frac{\text{weight of water}}{\text{density of water}} \qquad \text{(II-6)}$$

Standardization of Thermocouples

The two platinum-10% rhodium thermocouples, T_p, Figure 1, were standardized by comparison with a standard platinum-10% rhodium thermocouple obtained from the National Bureau of Standards. For the

calibration, the Bureau of Standards thermocouple and one of the thermocouples, T_p, were inserted in a 6-in. length of four-hole alundum thermocouple tubing and connected through an ice-water reference cold-junction to a Rubicon K-2 potentiometer. The alundum tubing containing the two thermocouples was introduced into a hole, 2 in. long, in the center of a 4-in. length of 1.5-in. copper rod. The rod with the thermocouples was then placed in the center of winding B of the differential temperature furnace and heated to various constant temperatures. The thermocouple potentials were measured to the nearest microvolt. Potential-difference measurements for the thermocouples were taken at 200-degree intervals as the temperature of the copper rod was increased from 200° to 1000° C. Measurements were also taken at intermediate temperatures as the temperature of the copper rod was decreased. The aforementioned procedure was employed with both the thermocouples, T_p. A correction table was then set up for each thermocouple.

Analysis of Samples

Polonium

At the completion of a run with polonium, all of the polonium was collected at the end B of the quartz cell by placing the bulb end, A, in a tube furnace and heating to 950° C. After the system had cooled, a 2-in. length of the tube end, B, containing the polonium was flame-sealed off. The total amount of polonium used in the run was determined by a calorimetric measurement of the heat emission. From the accurate absolute

measurement of the energy of the alpha particle of polonium-210 (5.2984 Mev.) made by Lewis and Bowden,[41] the heat generated per curie of polonium can be calculated. Thus a very accurate quantitative determination of the polonium content was possible by simple calorimetry. The determinations made on the polonium samples were reproducible to within ±0.001 curie.

Tellurium

At the completion of the runs with tellurium, all of the tellurium was collected at the end B of the quartz cell by placing the bulb end, A, in a tube furnace and heating to 750° C. After the system had cooled, a file mark was made approximately 2 in. up from the tube-end of the cell and the cell broken open. The tellurium content was determined by the volumetric-analysis method described by J. Grant.[42] In this procedure the tellurium metal was first converted to tellurous acid. The tellurous acid was then oxidized by addition of an excess of standard dichromate solution,

$$3H_2TeO_3 + K_2Cr_2O_7 + 8HCl \rightarrow 3H_2TeO_4 + 2KCl + 2CrCl_3 + 4H_2O, \quad (II-7)$$

and the excess dichromate determined with standard ferrous sulfate solution, using diphenylamine as an internal indicator.

Numerous experimental determinations were carried out on standard tellurium samples containing approximately 0.005 g. of tellurium to gain familiarity with the procedure and to determine the accuracy of the method. Results accurate to within ± 3 per cent were obtained, consistently.

Selenium

At the completion of the runs with selenium, all of the selenium was collected at end B of the cell and the cell broken open according to the procedure used for tellurium. The selenium content was determined by the volumetric-analysis method of Coleman and McCrosky.[43] In this procedure, the selenium was first converted to selenious acid. The selenious acid was then reduced by addition of an excess of standard thiosulfate solution,

$$4Na_2S_2O_3 + H_2SeO_3 + 4HCl \dashrightarrow 2Na_2S_4O_6 + 4NaCl + 3H_2O + Se, \quad (II-8)$$

and the excess thiosulfate determined by titration with standard iodine solution, using the usual starch indicator.

Several experimental determinations were carried out on standard selenium samples of approximately 0.005 g., to gain familiarity with the procedure and to determine the accuracy of the method. Results accurate to within ± 1 per cent were obtained, consistently.

The selenium pellet used in the preparation of the selenium sample had been weighed on a microbalance. The value obtained by the volumetric analysis agreed with the weight determination to within ± 0.5 per cent.

Errors

The main sources of errors are considered to be the following:

(1) the statistical variation of the counting rate (± 1%);

(2) the uncertainty in the amount of absorption of polonium on the walls of the quartz bulb (± 1% for measurements at temperatures

of T_B below 450°C.);

(3) the uncertainty in the actual temperature of the condensed polonium due to the heat emission of polonium (± 1° C.); and

(4) the uncertainty in the vapor density of polonium due to the depression of vapor pressure by the lead impurity (± 3%).

It is thought that the error in the vapor density measurements for polonium is not greater than 10 per cent. The error for the tellurium and selenium vapor density determinations should not be greater than 5 per cent.

PART III

Results and Calculations

The experimental data for the vapor-density runs on selenium, tellurium, and polonium are recorded in Tables I through XVI.

The data for the selenium were taken over the temperature range from 280.0° to 540.5° C. for the condensed phase and from 308.4° to 728.4° C. for the vapor. The product, (θT_A), was calculated for each determination and the log (θT_A) was plotted versus $1/T_B$. The points show wide variations from the linear plot of the data obtained for the value of $(T_A - T_B)$ less than 50°, as would be expected for a vapor which undergoes dissociation. The curve appears in Figure 12.

The data for the tellurium sample were taken over the temperature range from 483.2° to 756.9°C. for the condensed phase and from 512.1° to 880.0°C. for the vapor. The product, (θT_A), was calculated for each determination and the log (θT_A) was plotted versus $1/T_B$. A straight line was obtained as predicted by equation (I-7), suggesting that the vapor contained a single molecular species. Assuming a diatomic molecule, the vapor pressure, P, was calculated and the log P was plotted versus $1/T_B$. These curves appear in Figures 13, 14, and 15.

Measurements on polonium include data for polonium samples with decay times of 0 to 2 days, 6 to 7 days, 38 to 39 days, and 70 to

73 days. The data for the polonium samples with decay times of 0 to 2 days were taken over the temperature range from 382.3° to 610.0°C. for the condensed phase and from 422.3° to 1013.0°C. for the vapor. The product of vapor density-vapor temperature, (θT_A), was calculated for each determination and the log (θT_A) was plotted versus $1/T_B$. A straight line was obtained as predicted by equation (I-7), suggesting that the vapor contained one molecular species. The vapor pressure, P, was calculated, assuming diatomic molecules in the vapor, and the log P plotted versus $1/T_B$. These curves appear in Figures 16, 17, and 18. Values for (θT_A) and vapor pressure were also calculated for the data of runs made with polonium samples with decay times of 6 to 73 days. The curves for the log (θT_A) plotted versus $1/T_B$ and the log P plotted versus $1/T_B$ for these runs appear in Figures 19, 20, and 21.

Treatment of Counting Data

Because the time for the individual runs varied from 2 days to over 30 days, it was necessary to employ a counting standard, as mentioned previously, in order to compensate for radioactive decay and changes in counter response during a run.

The counting data recorded for each temperature consisted of a total of six counting rates taken with the scintillation counters A and B. The counting rates taken with counter A were: (1) the counting rate of the vapor at A, (2) the counting rate of the vapor plus the counting

standard at A, and (3) the counting rate of the vapor at A. With the scintillation counter B, the following counts were taken: (4) the counting rate of the condensed material at B, (5) the counting rate of the condensed material and the counting standard at B, and (6) the counting rate of the condensed material at B. All of the counts taken with counter A are identified by the letter A; those taken with counter B are identified by the letter B. Different subscripts are used to differentiate between the various counting rates as follows:

A_o = observed counting rate of vapor, determined as the average of counts (1) and (3) above.

B_o = observed counting rate of condensed phase, determined as the average of counts (4) and (6) above.

A_s = counting rate for counting standard in position A. This value was determined as the difference between counts (2) and A_o above.

B_s = counting rate for counting standard in position B. This value was determined as the difference between counts (5) and B_o above.

A_{sv} = counting rate of counting standard when the material in the quartz cell was completely vaporized.

A_b, B_b = counting rate for normal background due to cosmic radiation, noise in photomultiplier tubes and electronic circuits, etc.

A_{bB}, B_{bB} = counting rate when quartz cell, with all of active material collected at end B, was positioned in differential-temperature furnace prior to heating.

The observed counting rates were first corrected to the counting standards as follows:

$$A_c = A_o \frac{A_{sv}}{A_s} \qquad \text{(III-1)}$$

$$B_c = B_o \frac{B_{sv}}{B_s} \qquad \text{(III-2)}$$

where

A_c = observed counting rate at A corrected to counting standard, and

B_c = observed counting rate at B corrected to counting standard.

The counting rate for the vapor was then corrected for background. In this connection it was necessary to consider two background corrections. The correction, A_b, due to normal background; and the correction, A_p, due to penetration through the lead shielding of a fraction of the radiation from the condensed phase. The equations developed for calculating these corrections are:

$$A_{bc} = A_c - A_b - A_p, \qquad \text{(III-3)}$$

where

$$A_p = (B_c - B_b) \frac{(A_{bB} - A_b)}{(B_{bB} - B_b)} \qquad \text{(III-4)}$$

in which

A_{bc} = counting rate for vapor corrected to counting standard and for background.

The correction, A_p, was of importance only for measurements made at low vapor pressures.

Calculation of Vapor Density

The calculation of vapor density for the various temperatures was made by the following equation:

$$\theta = A_{bc} \frac{W}{V A_v} \qquad \text{(III-5)}$$

in which

θ = vapor density, g./cc.

W = total weight of material in quartz cell, g.

V = volume of cell, cc.

A_v = counting rate when material completely vaporized. (corrected to counting standard and for background)

Calculation of Molar Heat of Vaporization

In Figures 13 and 16 plots of logarithms of (θT_A) versus the reciprocals of the absolute temperatures, T_B, yield straight lines as predicted by equation (I-7).

The equations for the lines were obtained by the method of least squares[44] with the assumption that the liability of error is limited to the dependent variable, log (θT_A), and all values have equal weights. The

molar heat of vaporization was then calculated by multiplying the value for the slope of the line by -0.2185. The standard error was also calculated.[45] The values for the heats of vaporization for polonium and tellurium are 26.31 ± 0.15 and 27.35 ± 0.13 kcals./mole, respectively.

Calculation of Vapor Pressure

From equation (I-2), the vapor pressure can be expressed as a function of the vapor density by the following:

$$P = \theta T_A \frac{R}{M}. \qquad \text{(III-6)}$$

Because the results of this investigation suggest that both polonium and tellurium vapors contain a single molecular species, then, assuming diatomic molecules in the vapors, equation (III-6) can be used to calculate values of vapor pressure for various temperatures, T_B. The values obtained are tabulated in Tables VI, VII, IX, and X. The logarithms of the calculated vapor pressures are plotted versus the reciprocals of the absolute temperatures, T_B, in Figures 14 and 17.

Calculation of Normal Boiling Point

The normal boiling point is that temperature of the condensed phase for which its equilibrium vapor pressure is 760 mm. To determine the normal boiling point of polonium and tellurium, the general equation,

$$\log P = \frac{A}{T_B} + B \qquad \text{(III-7)}$$

was used. The constants, A and B, were evaluated from the data in Tables VI, VII, IX, and X by the method of least squares. The standard

error was determined for the constants.

The normal boiling points for polonium and tellurium were then calculated by setting P = 760 mm. and solving equation (III-7) for T_B. These calculated normal boiling points are 946.5° ± 10.2° C. and 982.5° ± 7.4° C., respectively.

Calculation of Trouton's Constant

The Trouton's constant is equal to the entropy of vaporization of a mole of substance at its normal boiling point. It was determined by the following equation:

$$\text{Trouton's constant} = \frac{\Delta H_v}{T_b} \qquad \text{(III-8)}$$

where

ΔH_v = molar heat of vaporization, cals.

T_b = normal boiling point, deg. Kelvin.

The calculated values of Trouton's constant for polonium and tellurium are 21.6 and 21.8 cal. /deg., respectively. These values suggest that there is no unusual dissociation in liquid polonium and tellurium at the respective boiling points.

Calculation of Association Number

The association number, is defined by the expression:

$$a = \frac{M_a}{S}, \qquad \text{(III-9)}$$

where

M_a = the apparent molecular weight of vapor as determined by equation (I-2), and

S = the atomic weight of the particular element.

For the calculation of the apparent molecular weight at the various temperatures the vapor-pressure values required were taken from the works of Brooks.[4, 6]

TABLE I

Experimental Data for Selenium, Run No. 1
6.25×10^{-3} g. Selenium 14.71 cc. cell

T_A, °K	T_B, °K	θ*, 10^6 g./cc.	θT_A, 10^3 g. deg./cc.	a**
644.1	614.2	12.4	8.02	6.86
705.9	612.2	9.09	6.42	5.82
680.1	649.4	25.7	17.5	5.44
717.8	690.9	69.9	50.2	5.37
724.4	702.1	82.6	59.8	4.91
764.4	702.4	75.4	57.6	4.73
795.6	702.6	64.5	51.3	4.16
888.6	702.1	37.2	33.1	2.72

* Vapor Density

** Association Number

TABLE II

Experimental Data for Selenium, Run No. 2
6.25×10^{-3} g. Selenium 14.71 cc. cell

T_A, °K	T_B, °K	θ*, 10^6 g./cc.	θT_A, 10^3 g. deg./cc.	a**,
723.0	654.2	25.5	18.4	5.05
764.8	654.0	18.7	14.3	3.92
680.2	656.3	31.7	21.5	5.57
795.3	656.7	16.3	13.0	3.32
698.1	672.4	46.7	32.6	5.51
733.1	706.6	96.8	71.0	5.24
786.0	766.6	310.	244.	5.05
874.9	767.0	185.	162.	3.35
949.9	765.1	118.	112.	2.40
1002.5	775.1	128.	128.	2.25

* Vapor Density

** Association Number

TABLE III

Experimental Data for Selenium, Run No. 3

6.25×10^{-3} g. Selenium 14.71 cc. cell

T_A, °K	T_B, °K	θ*, 10^6 g./cc.	θT_A, 10^3 g. deg./cc.	a**,
581.5	553.1	1.18	0.68	4.59
659.2	556.9	1.01	0.66	3.89
691.3	661.2	36.1	25.0	5.64
760.8	665.4	26.9	20.5	4.68
866.2	687.3	25.7	22.2	2.60
955.0	746.1	77.5	74.0	2.31
957.0	776.0	146.	140.	2.44

* Vapor Density

** Association Number

TABLE IV

Experimental Data for Selenium, Run No. 4
6.25×10^{-3} g. Selenium 14.71 cc. cell

T_A, °K	T_B, °K	ϱ*, 10^6 g./cc.	ϱT_A, 10^3 g. deg./cc.	a**,
740.6	623.0	8.07	5.98	3.94
741.6	652.0	19.9	14.8	4.30
805.7	672.6	24.6	19.8	3.35
743.6	677.5	44.0	32.8	4.89
846.3	680.5	23.1	19.6	2.73
743.6	698.3	77.9	57.9	5.21
805.6	701.3	58.2	46.9	3.94
844.9	707.8	49.3	41.7	3.02
742.9	711.6	113.	83.7	5.51
962.4	723.8	47.6	45.9	2.32
806.9	732.4	131.	106.	4.41
848.7	741.4	120.	102.	3.46
809.8	765.4	271.	220.	4.71
848.7	770.4	250.	212.	4.08
960.7	772.5	139.	133.	2.45
984.4	777.7	141.	139.	2.34
908.2	795.0	298.	270.	3.29
981.4	797.1	218.	214.	2.52
984.2	797.3	218.	215.	2.50
985.0	813.6	291.	287.	2.51

712

* Vapor Density

** Association Number

TABLE V

Experimental Data for Selenium Vapor at Constant Pressure

6.25×10^{-3} g. Selenium 14.71 cc. cell

T_A, °K	T_B, °K	ΔT $(T_A - T_B)$	θ*, 10^6 g./cc.	θT_A, 10^3 g. deg./cc.
644.1	614.2	29.9	12.4	8.02
705.9	612.2	93.7	9.09	6.42
680.2	656.3	23.0	31.7	21.5
723.0	654.2	68.8	25.5	18.4
764.8	654.0	110.8	18.7	14.3
795.3	656.7	138.6	16.3	13.0
698.1	672.4	25.7	46.7	32.6
805.7	672.6	133.1	24.6	19.8
724.4	702.1	22.3	82.6	59.8
764.4	702.4	62.0	75.4	57.6
795.6	702.6	93.0	64.5	51.3
888.6	702.1	186.5	37.2	33.1
786.0	766.6	19.4	310.	244.
799.2	766.7	32.5	298.	238.
809.8	765.4	44.4	271.	220.
874.9	767.0	107.9	185.	162.
949.9	765.1	184.8	118.	112.
908.2	795.0	113.2	298.	270.
984.2	797.3	186.9	218.	215.

*Vapor Density

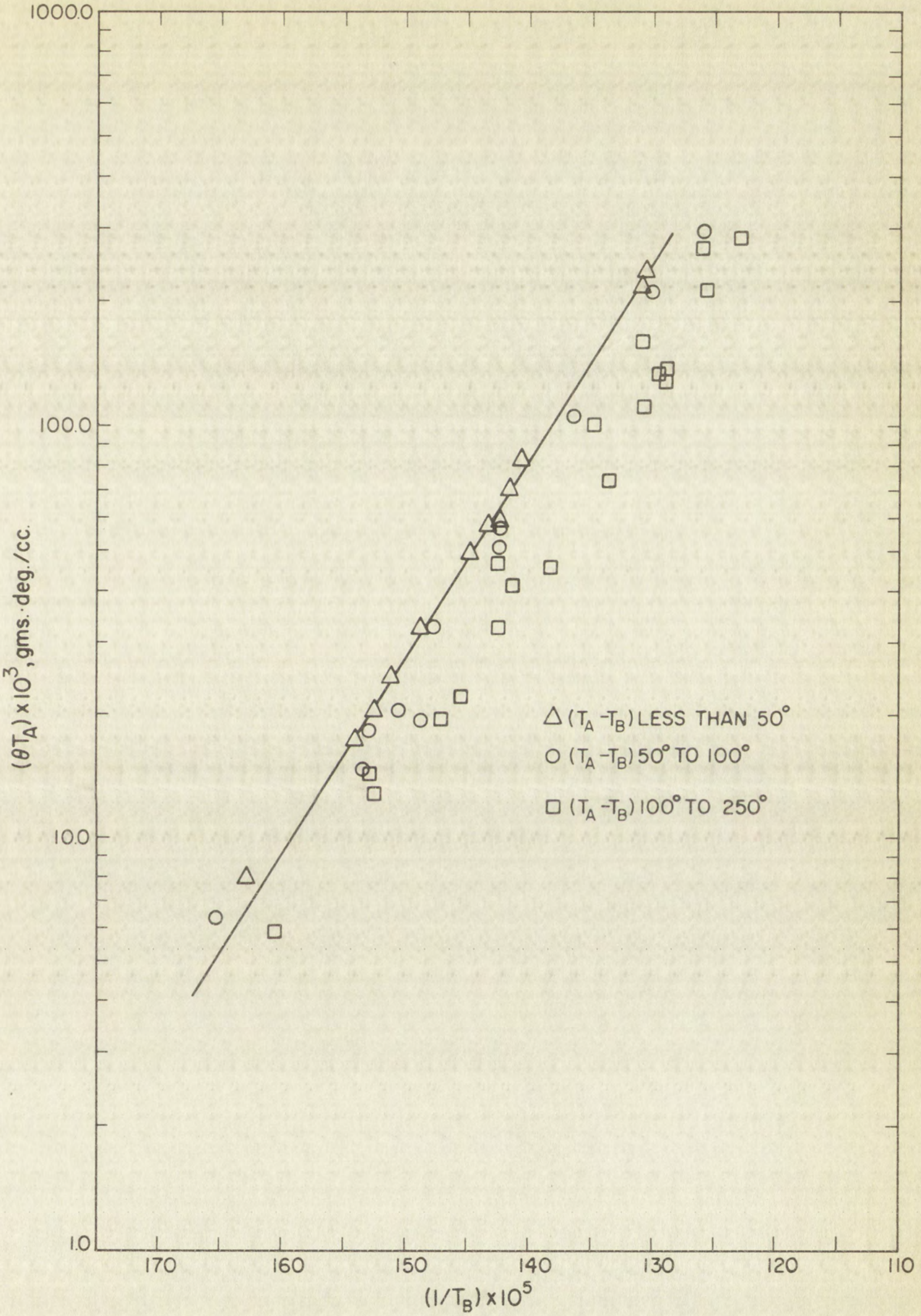

Figure 12. Log (θT_A) versus $1/T_B$ for Selenium.

TABLE VI

Experimental Data for Tellurium, Run No. 5
5.57×10^{-3} g. Tellurium 15.85 cc. cell

T_A, °K	T_B, °K	ϱ*, 10^6 g./cc.	ϱT_A, 10^3 g. deg./cc.	P**, mm. Hg
785.2	756.3	2.85	2.24	0.547
863.5	834.2	13.9	12.0	2.93
898.6	864.1	24.2	21.7	5.30
935.2	905.5	48.7	45.5	11.1
1052.1	912.6	47.7	49.9	12.2
979.6	949.9	96.6	94.6	23.1
1026.3	992.3	170.	174.	42.5
1060.8	1027.7	257.	273.	66.7

* Vapor Density

** Vapor Pressure Calculated for Te_2 Molecules

TABLE VII

Experimental Data for Tellurium, Run No. 6

5.57×10^{-3} g. Tellurium 15.85 cc. cell

T_A, °K	T_B, °K	θ*, 10^6 g./cc.	θT_A, 10^3 g. deg./cc.	P**, mm. Hg
826.0	796.2	6.95	5.74	1.40
942.9	917.2	57.2	53.9	13.2
1053.9	917.2	49.9	52.6	12.9
1148.1	918.1	46.4	53.3	13.0
1253.0	1002.3	153.	190.	46.4
1153.3	1027.3	231.	266.	65.0
1060.6	1030.0	274.	291.	71.1

* Vapor Density

** Vapor Pressure Calculated for Te_2 Molecules

TABLE VIII

Experimental Data for Tellurium Vapor at Constant Pressure

5.57×10^{-3} g. Tellurium — 15.85 cc. cell

T_A, °K	T_B, °K	ΔT, $(T_A - T_B)$	θ, * 10^6 g./cc.	θT_A, 10^3 g. deg./cc.
942.9	917.2	25.7	57.2	53.9
1053.9	917.2	136.7	49.9	52.6
1148.1	918.1	230.0	46.4	53.3
1060.8	1027.7	33.1	257.	272.
1153.5	1027.3	126.2	231.	266.

* Vapor Density

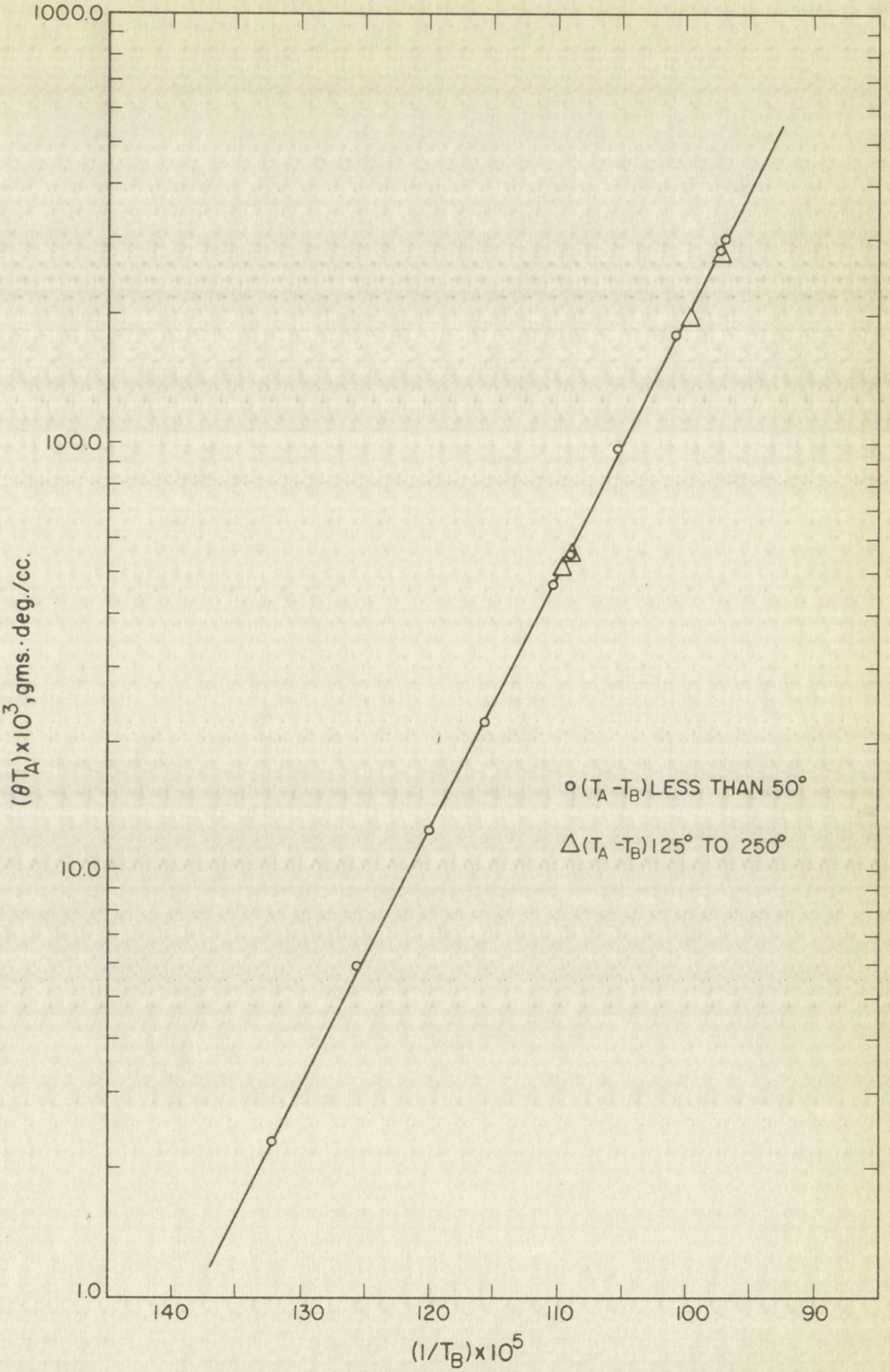

Figure 13. Log (θT_A) versus $1/T_B$ for Tellurium.

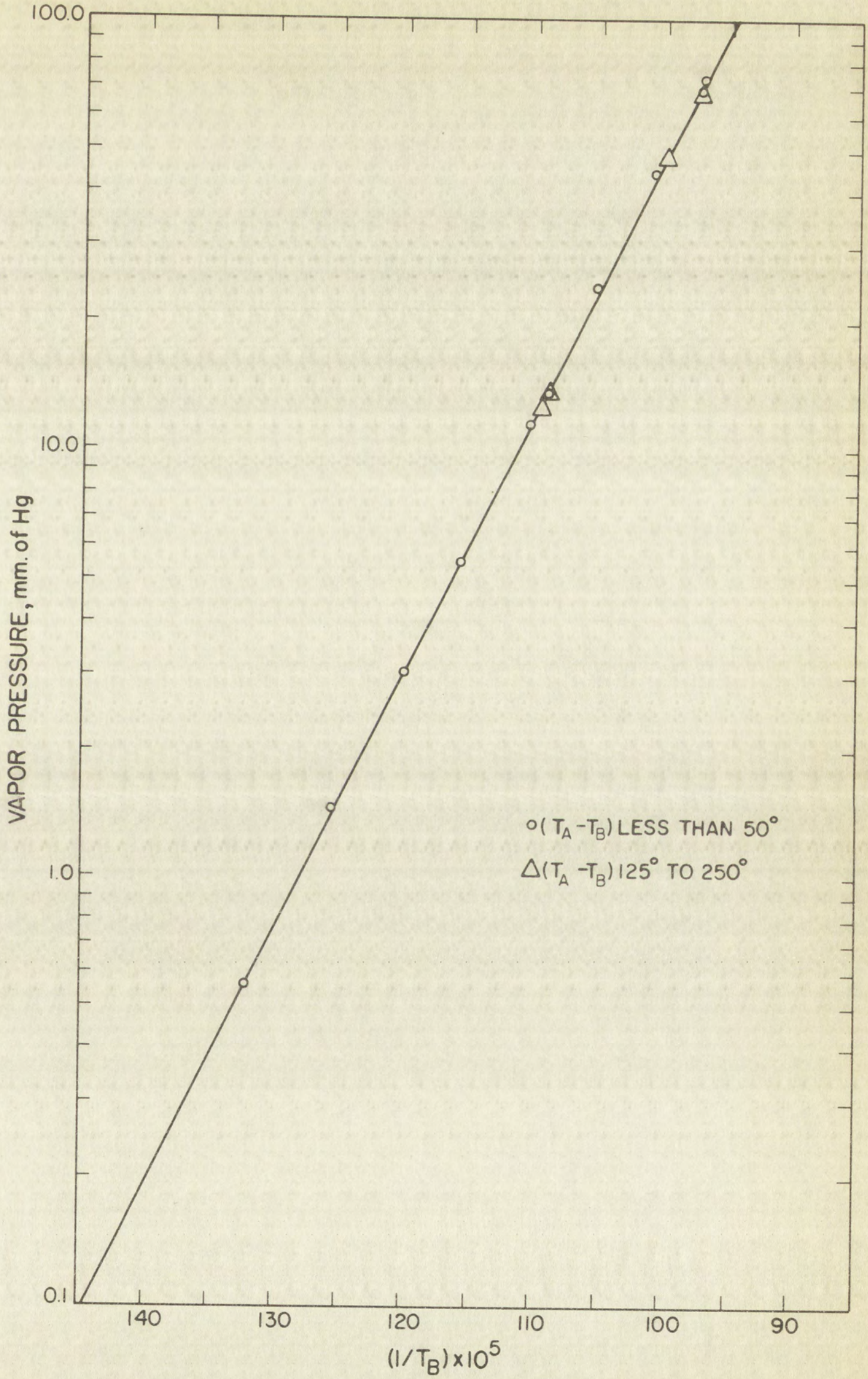

Figure 14. Log P versus $1/T_B$ for Tellurium.

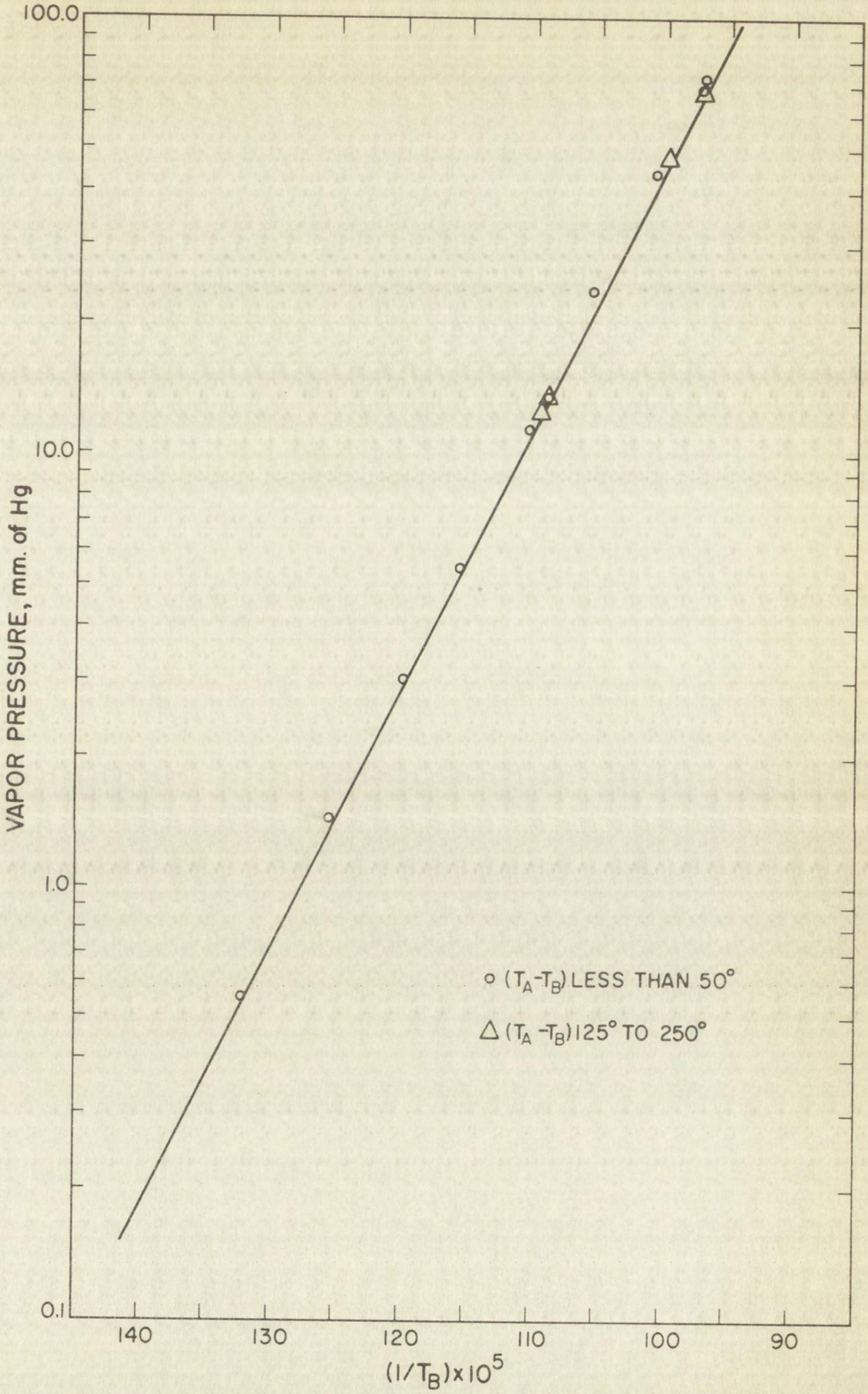

Figure 15. Tellurium Data Fitted to Brooks[4] Curve.

TABLE IX

Experimental Data for Polonium with 0 to 1 Atomic Per Cent Lead,
Run No. 7

5.32×10^{-4} g. Polonium 13.83 cc. cell

T_A, °K	T_B, °K	θ*, 10^6 g./cc.	θT_A, 10^3 g. deg./cc.	P**, mm. Hg
695.4	655.4	0.65	0.45	0.067
716.9	673.9	1.04	0.76	0.111
731.0	691.0	1.74	1.27	0.188
771.8	730.1	4.51	3.48	0.517
793.0	750.6	7.22	5.73	0.851
849.1	804.3	22.1	18.8	2.78
870.8	827.0	31.1	27.1	4.02

* Vapor Density

** Vapor Pressure Calculated for Po_2 Molecules

TABLE X

Experimental Data for Polonium with 0 to 1 Atomic Per Cent Lead, Run No. 8

1.88×10^{-3} g. Polonium — 11.36 cc. cell

T_A, °K	T_B, °K	θ*, 10^6 g./cc.	θT_A, 10^3 g. deg./cc.	P**, mm. Hg
794.8	727.5	4.05	3.22	0.478
827.6	766.1	10.9	9.05	1.34
834.7	767.5	10.7	8.96	1.33
1100.4	809.4	20.7	22.8	3.39
1286.1	811.2	17.4	22.4	3.33
872.4	812.3	25.7	22.4	3.33
907.6	845.4	48.4	43.9	6.52
925.6	858.9	55.5	51.3	7.62
953.0	883.1	84.2	80.2	11.9

* Vapor Density

** Vapor Pressure Calculated for Po_2 Molecules

TABLE XI

Experimental Data for Polonium Vapor at Constant Pressure

1.88×10^{-3} g. Polonium 11.36 cc. cell

T_A, °K	T_B, °K	ΔT $(T_A - T_B)$	θ,* 10^6 g./cc.	θT_A, 10^3 g. deg./cc.
872.4	812.3	60.1	25.7	22.4
1100.4	809.4	291.0	20.7	22.8
1286.1	811.2	474.9	17.4	22.4

* Vapor Density

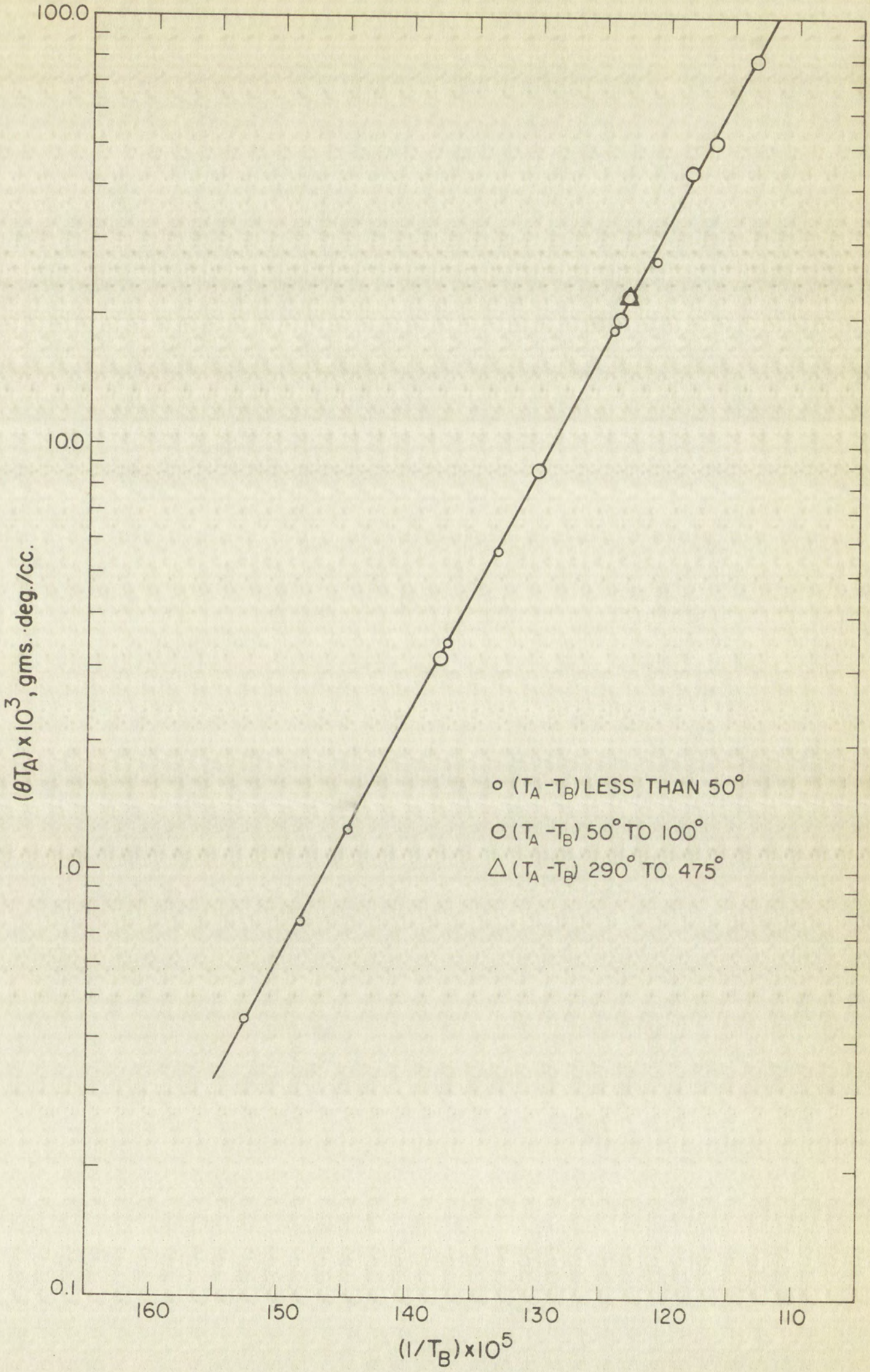

Figure 16. Log (θT_A) versus $1/T_B$ for Polonium with 0 to 1 Atomic Per Cent Lead.

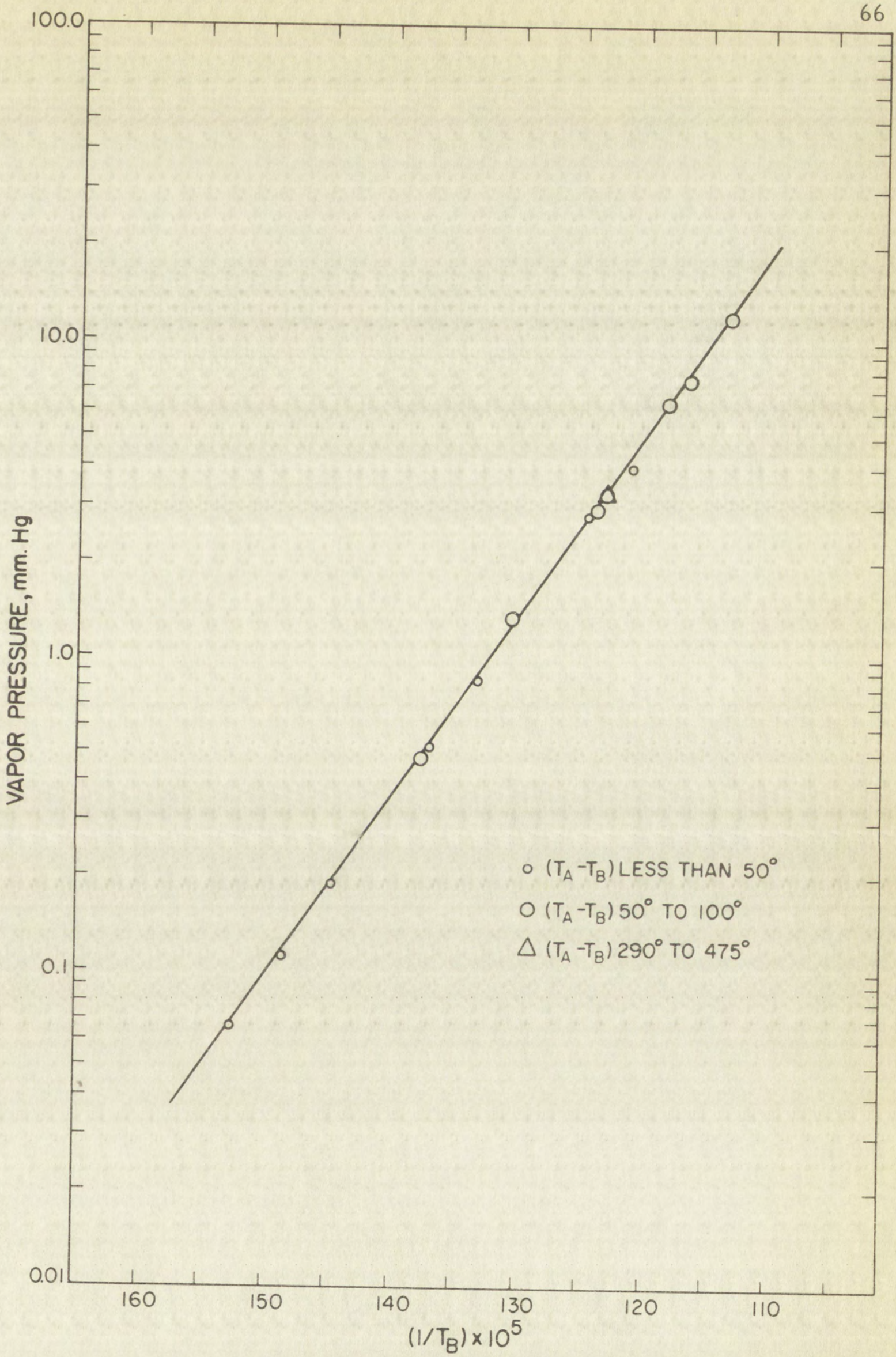

Figure 17. Log P versus $1/T_B$ for Polonium with 0 to 1 Atomic Per Cent Lead.

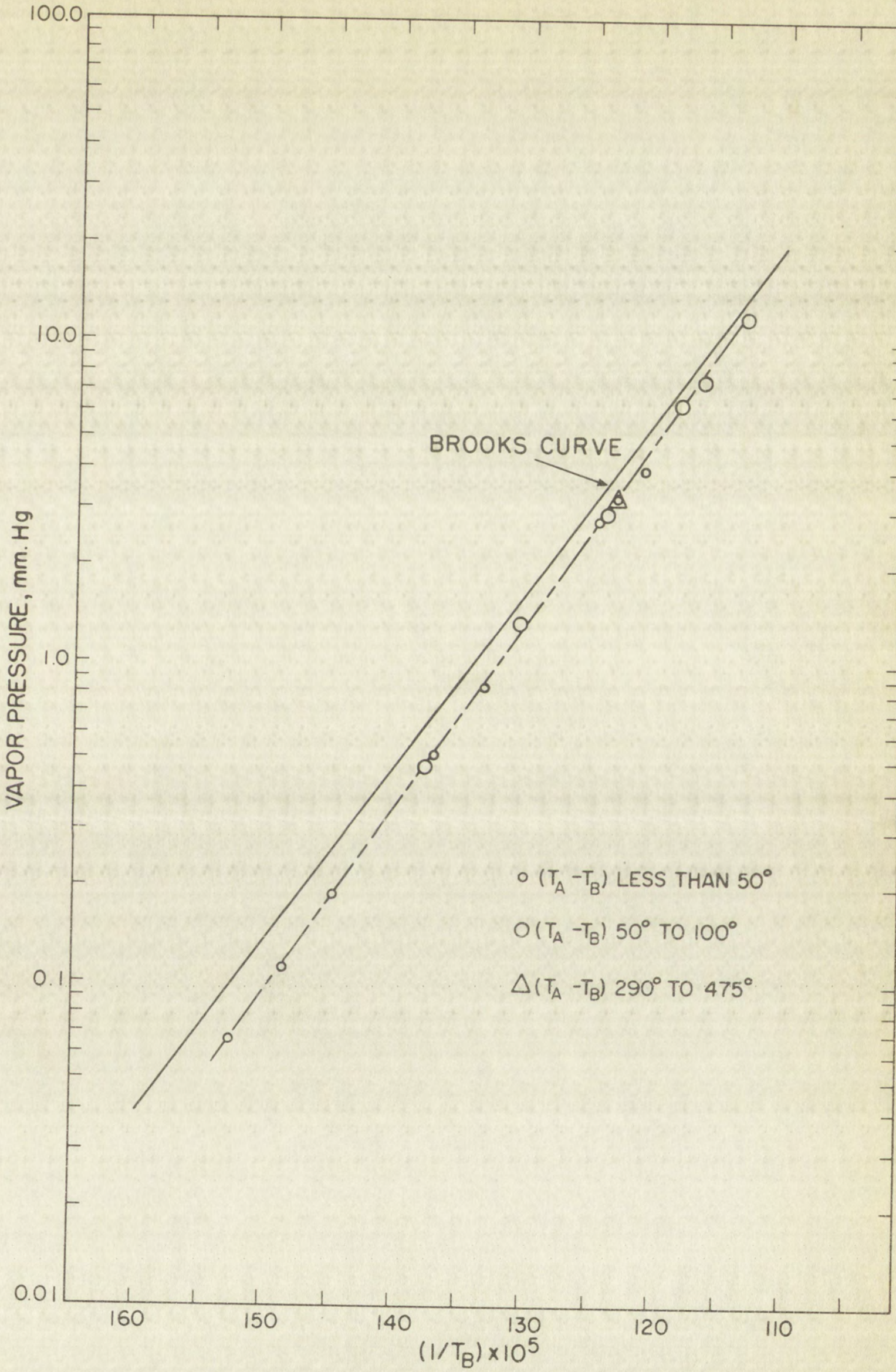

Figure 18. Calculated Data for Polonium Fitted to Brooks[6] Curve.

TABLE XII

Experimental Data for Polonium with 3 to 3.5 Atomic Per Cent Lead,
Run No. 9

3.97×10^{-4} g. Polonium — 13.95 cc. cell

T_A, °K	T_B, °K	θ*, 10^6 g./cc.	θT_A, 10^3 g. deg./cc.	P**, mm. Hg
740.9	676.0	1.04	0.77	0.115
751.2	708.2	2.40	1.80	0.267
770.4	723.8	3.44	2.65	0.394
807.4	763.2	8.37	6.76	1.00
828.5	781.6	12.0	10.0	1.48
886.7	838.8	23.4	20.8	3.08
1125.9	859.1	20.6	23.2	3.44
990.7	945.6	27.2	26.9	4.00
1004.0	958.8	27.6	27.7	4.11

* Vapor Density

** Vapor Pressure Calculated for Po_2 Molecules

TABLE XIII

Experimental Data for Polonium with 17 to 17.8 Atomic Per Cent Lead,
Run No. 10

3.97×10^{-4} g. Polonium 13.95 cc. cell

T_A, °K	T_B, °K	θ*, 10^6 g./cc.	θT_A, 10^3 g. deg./cc.	P**, mm. Hg
747.3	706.7	1.05	0.79	0.117
791.3	748.3	2.90	2.30	0.341
833.6	786.3	5.92	4.94	0.733
849.5	807.1	7.55	6.41	0.953
900.5	853.9	11.1	10.0	1.49
949.9	908.1	14.7	14.0	2.08
983.3	944.2	16.5	16.2	2.41
1089.2	1045.4	20.8	22.7	3.37
1142.1	1096.5	23.3	26.7	3.96

* Vapor Density

** Vapor Pressure Calculated for Po_2 Molecules

TABLE XIV

Experimental Data for Polonium with 29 to 31 Atomic Per Cent Lead,
Run No. 11

3.97×10^{-4} g. Polonium — 13.95 cc. cell

T_A, °K	T_B, °K	θ*, 10^6 g./cc.	θT_A, 10^3 g. deg./cc.	P**, mm. Hg
754.2	709.6	0.28	0.21	0.031
778.8	735.7	0.46	0.35	0.053
808.7	767.5	1.03	0.83	0.123
831.3	788.5	1.54	1.28	0.190
863.1	819.0	2.41	2.08	0.309
893.1	853.1	3.64	3.25	0.483
927.6	882.8	4.98	4.62	0.686
977.4	931.5	6.62	6.47	0.961
998.0	955.1	8.04	8.02	1.19
1041.7	996.6	9.84	10.3	1.52
1112.9	1066.3	13.3	14.8	2.19
1199.1	1149.3	17.4	20.8	3.09
1271.9	1223.5	19.7	25.1	3.73

* Vapor Density

** Vapor Pressure Calculated for Po_2 Molecules

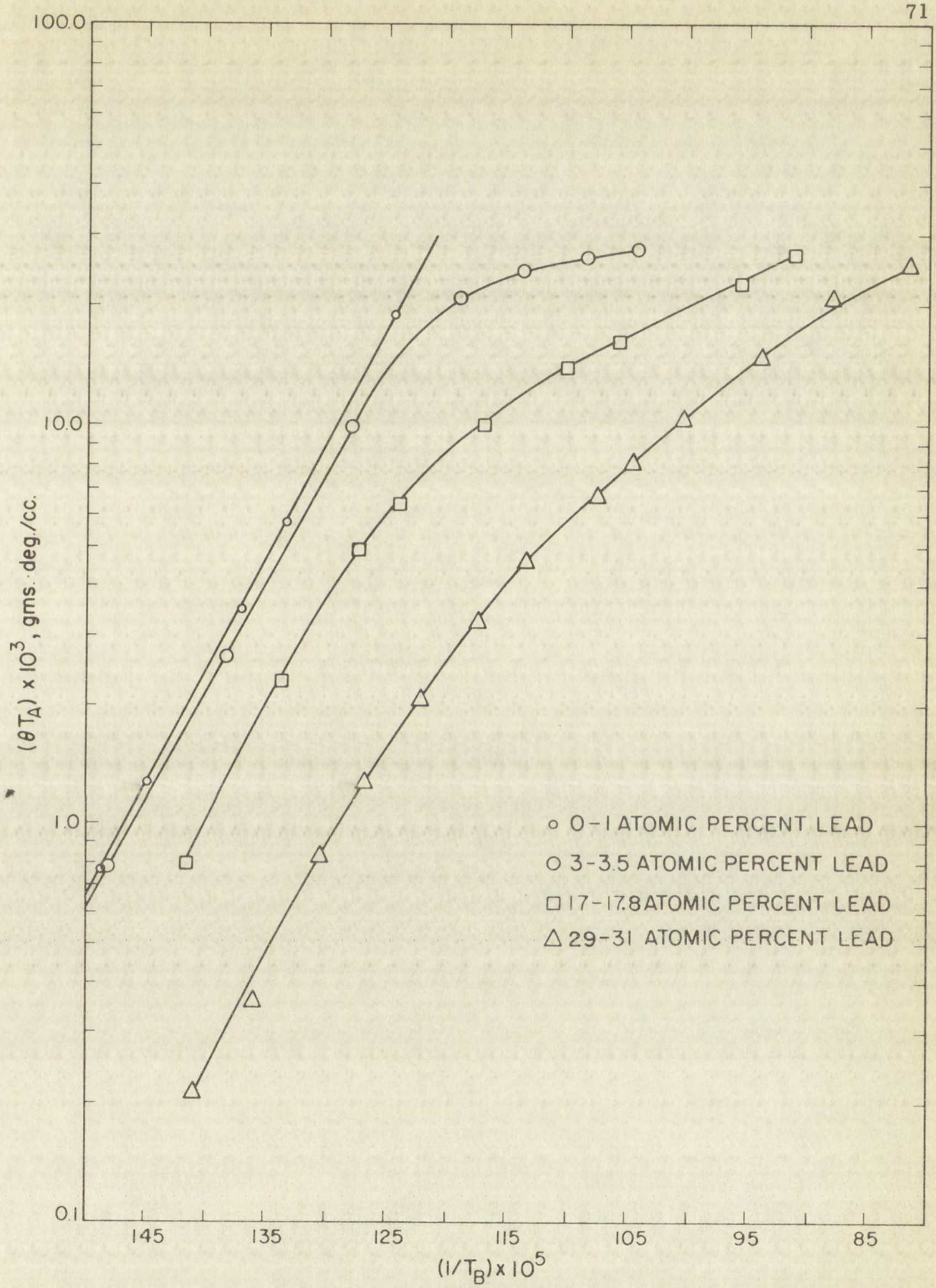

Figure 19. Log (θT_A) versus $1/T_B$ for Polonium with Various Lead Content.

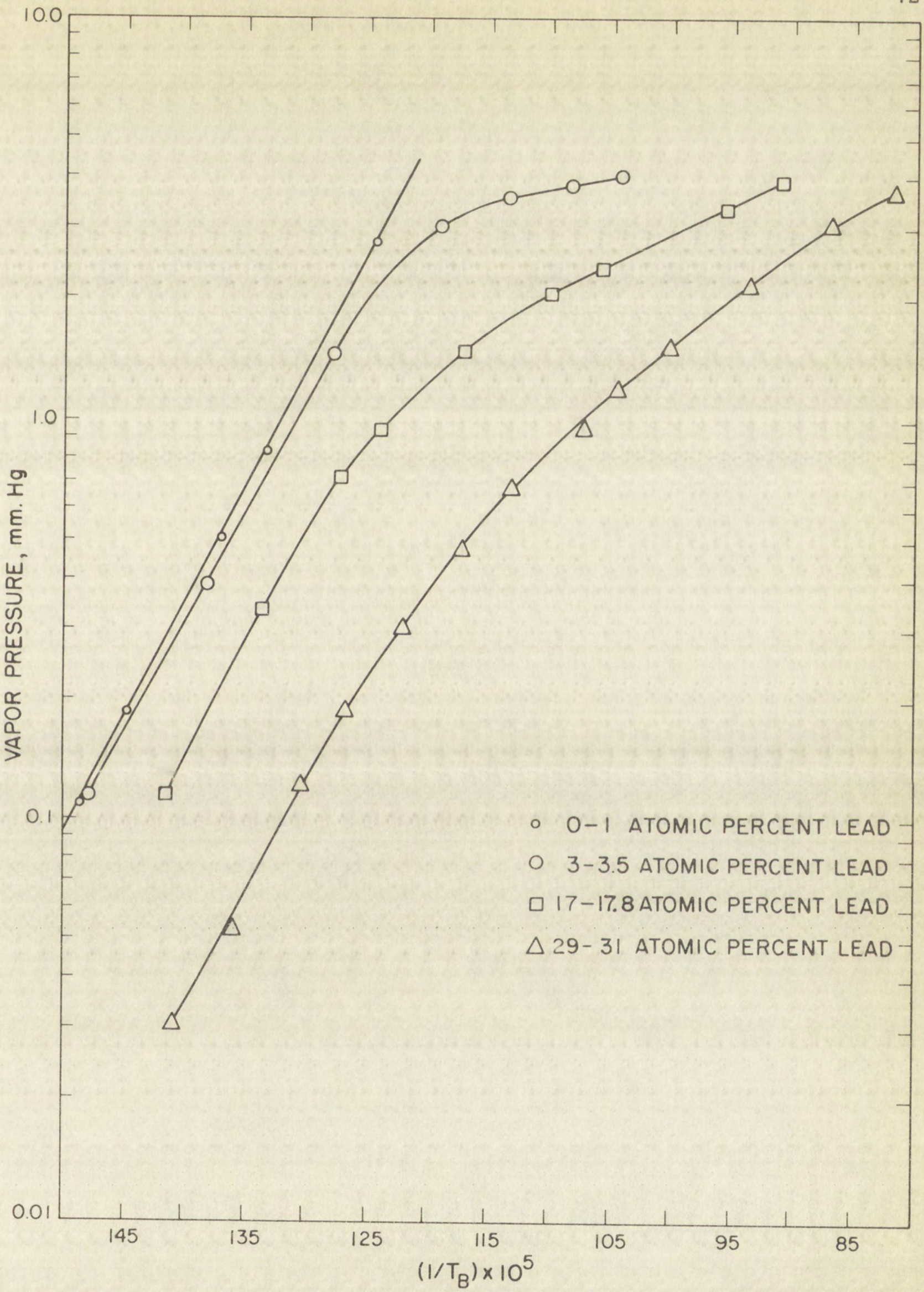

Figure 20. Log P versus $1/T_B$ for Polonium with Various Lead Content.

TABLE XV

Experimental Data for Polonium with 3 to 3.5 Atomic Per Cent Lead,
Run No. 12

1.83×10^{-3} g. Polonium — 11.36 cc. cell

T_A, °K	T_B, °K	θ*, 10^6 g./cc.	θT_A, 10^3 g. deg./cc.	P**, mm. Hg
760.0	692.1	1.62	1.23	0.183
921.7	797.8	17.0	15.7	2.33
1279.0	883.6	54.4	69.6	10.3
971.4	903.3	99.8	96.9	14.4
1282.4	927.3	91.2	117.	17.4
1001.2	929.7	123.4	123.5	18.3
1021.0	949.6	132.	135.	20.1
1042.9	987.6	149.	156.	23.1

* Vapor Density

** Vapor Pressure Calculated for Po_2 Molecules

TABLE XVI

Experimental Data for Polonium with 3 to 3.5 Atomic Per Cent Lead,
Run No. 13

5.14×10^{-4} g. Polonium 13.83 cc. cell

T_A, °K	T_B, °K	θ*, 10^6 g./cc.	θT_A, 10^3 g. deg./cc.	P**, mm. Hg
752.7	711.3	2.62	1.97	0.293
777.6	752.0	7.31	5.68	0.844
834.5	791.7	15.3	12.8	1.89
906.0	863.9	30.7	27.8	4.13
951.2	907.7	33.5	31.9	4.74
987.9	944.1	34.4	34.0	5.05

* Vapor Density

** Vapor Pressure Calculated for Po_2 Molecules

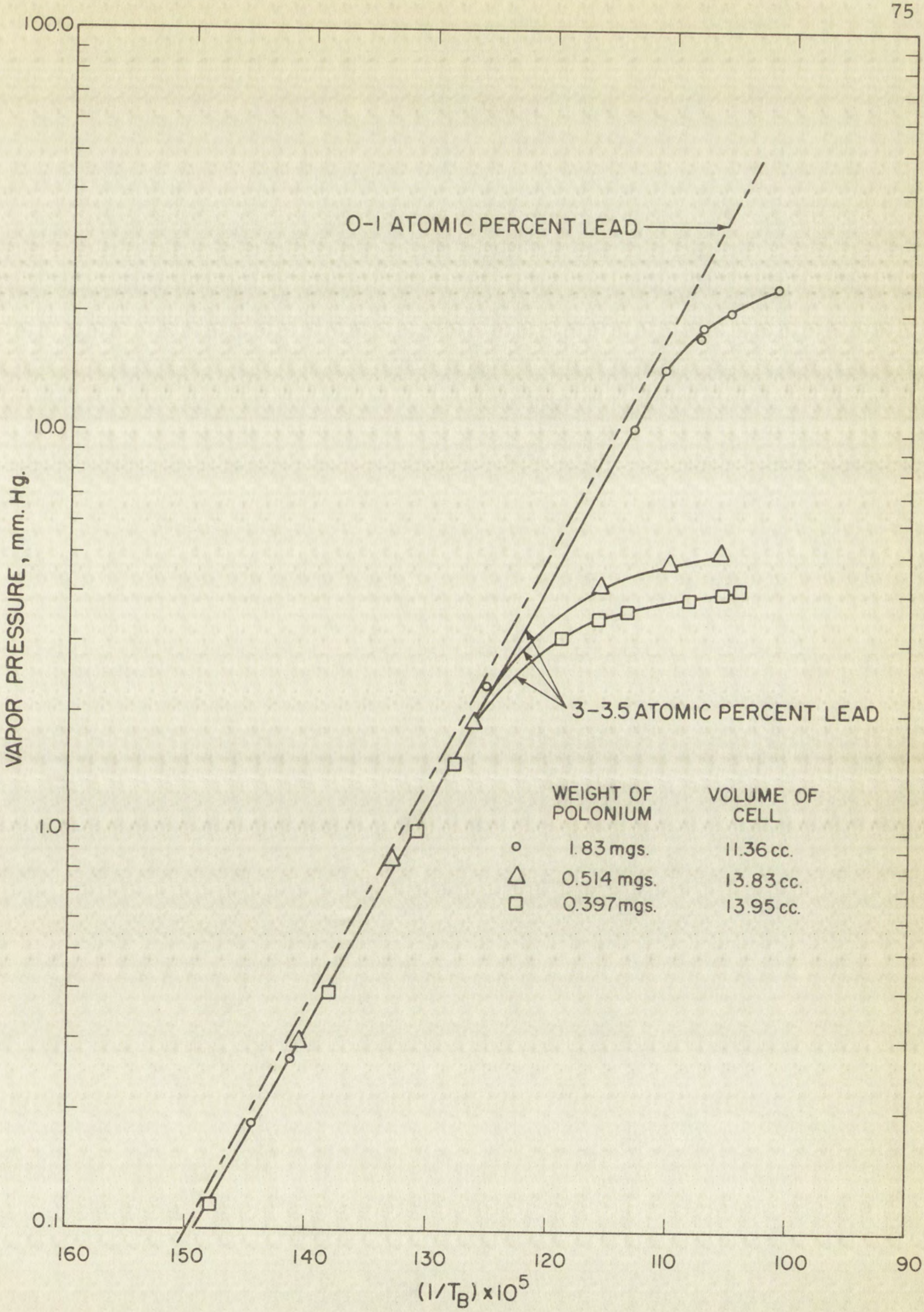

Figure 21. Log P versus $1/T_B$ for Polonium with 3 to 3.5 Atomic Per Cent Lead.

PART IV

Discussion

Variation of the (θT_A) Values with Temperature of Selenium Vapor

The data for the density of the selenium vapor as determined by four experimental runs made at various temperatures and pressures are reported in Tables I, II, III, and IV. These tables also include values for the vapor density-vapor temperature product, θT_A, and the association number, a, calculated for the various data.

For the determination of the association number, the vapor pressures corresponding to the temperatures, T_B, of the condensed phase were calculated with the equation:

$$\log P = \frac{-4989.5}{T_B} + 8.0886, \qquad \text{(IV-1)}$$

where

P = vapor pressure of liquid selenium, mm.

T_B = temperature of liquid selenium, deg. Kelvin.

This equation was determined by Brooks[4] in his study of the variation of vapor pressure with temperature for selenium over the temperature range from 262.8° to 687.8° C. The calculated values for the association numbers were found to vary from 2.25 to 6.86, suggesting that the selenium vapor contained molecules larger than Se_6. Preuner and Schuff[46]

in their investigation of the variation of vapor density of selenium with vapor pressure over the temperature range from 550° to 800° C., found that the equilibrium $Se_6 = 3Se_2$ occurred in the vapor and suspected that equilibria involving other molecular species were also present. The results of this investigation substantiate the belief that the equilibria involves at least three molecular species. However, attempts to resolve the equilibria in the selenium vapor with the limited data obtained in this study were unsuccessful.

The logarithm of the product, θT_A, was plotted versus the reciprocal of the absolute temperature of the condensed phase in Figure 12. The values for the product, θT_A, are represented in this graph as the following three sets of data: (1) measurements in which the temperature difference $(T_A - T_B)$, was less than 50°C., (2) measurements in which $(T_A - T_B)$ was varied between 50° and 100°C., and (3) measurements in which $(T_A - T_B)$ was varied between 100° and 250°C. The data for the measurements in which $(T_A - T_B)$ was less than 50°C. were fitted to a straight line in Figure 12. It will be observed that as the temperature difference, $(T_A - T_B)$, was increased to between 50° and 100°C., all of the values obtained for (θT_A) are lower than the corresponding values from the curve. Further, as the temperature differential was increased to between 100° and 250°C., the values of (θT_A) become much lower than the corresponding values for the two previous sets of data. The resulting graph, Figure 12, of all of these data shows a very marked divergence from any linearity. A tabulation was also made of the (θT_A)

values obtained at constant pressure (i.e., constant T_B) for several different pressures. These data are recorded in Table V. An examination of this table shows that here again the values of (θT_A) decrease with increasing vapor temperatures at constant pressure in all cases. These results are in agreement with the predictions based on equation (I-3) for vapor in which dissociation occurs.

The magnitude of the variations of the values for (θT_A) with the temperature of the vapor at constant pressure indicate that this method of determining vapor densities can indeed be used to detect dissociation in a vapor in equilibrium with a liquid phase. Thus, if dissociation does occur in a vapor, the data obtained should indicate it in the following two ways:

(1) a plot of the logarithm of the values for (θT_A) versus the reciprocal of the absolute temperature of the condensed phase for measurements made at varying temperature differentials, ($T_A - T_B$), should show wide variations from a linear graph, and

(2) the values of (θT_A) for measurements made at constant pressure should decrease as the temperature of the vapor is increased.

Molar Heat of Vaporization, Normal Boiling Point, and Trouton's Constant for Tellurium

Two experimental runs were made on the tellurium sample. The data obtained for the density of the tellurium vapor at the various temperatures and pressures are reported in Tables VI and VII. The logarithm

of the product, (θT_A), was plotted versus the reciprocal of the absolute temperature of the condensed phase in Figure 13. Although the values of the product, (θT_A), were determined for measurements in which the temperature differential, $(T_A - T_B)$, was varied from 25.7° to 250.7°C., all of the data conform to a linear plot within the accuracy of the measurements. The experimental data for the values of the product, (θT_A), obtained at constant pressure are reported in Table VIII. The data in this table show that the product, (θT_A), remains constant (within the experimental error) for measurements made at constant pressure in which the temperature differential, $(T_A - T_B)$, was varied over wide limits. These results suggest that tellurium vapor consists of a single molecular species over the temperature range studied. The assumption that the vapor consisted entirely of diatomic molecules was based on results of Electron-diffraction studies of tellurium vapor at approximately 600°C.[47] Then, using equation (I-2), the corresponding vapor pressures were calculated from the values of (θT_A) for the various data. These vapor-pressure values are recorded in Tables VI and VII. The logarithm of the vapor-pressure values was plotted versus the reciprocal of the absolute temperature of the condensed phase. This curve is presented in Figure 14. The equation for the linear plot was solved by the method of least squares and the standard deviation for the slope and the intercept of the line determined:

$$\log P = \frac{-5976.9 \pm 27.8}{T_B} + 7.6409 \pm 0.0322 \qquad \text{(IV-2)}$$

where

P = vapor pressure of liquid tellurium, mm.

T_B = temperature of liquid tellurium, deg. Kelvin.

Using the above equation, values for the molar heat vaporization, the normal boiling point, and Trouton's constant were calculated. The value for the slope of the log P versus $1/T_B$ curve is identical to the slope of the log (θT_A) versus $1/T_B$ curve so either curve can be used to calculate the heat of vaporization. The calculated values are reported below:

Molar Heat of Vaporization	27.35 ± 0.13 kcals./mole
Normal Boiling Point	982.6° ± 7.4° C.
Trouton's Constant	21.8 cals./deg. mole.

It is of interest to compare the results of this investigation with those obtained by Brooks,[4] who determined the variation of vapor pressure with temperature, over essentially the same temperature range, by a Bourdon-type gage. In order to show the close agreement, the data determined in this investigation were fitted to the curve determined by Brooks. This graph is presented in Figure 15. Also the values for the molar heat of vaporization, normal boiling point, and Trouton's constant as determined in this investigation are compared to the values calculated by Brooks. These data are reported in Table XVII. This table also includes the values quoted by Yost and Russell.[48] The excellent agreement between the values obtained in this study and those obtained by Brooks

TABLE XVII

Comparison of Values for Heat of Vaporization, Normal Boiling Point, and Trouton's Constant Reported for Tellurium

	This Work	Brooks	Yost and Russell[48]
Heat of Vaporization, kcals./mole,	27.35 ± 0.13	27.26 ± 0.07	24.0
Normal Boiling Point, deg. C.,	982.5° ± 7.4°	989.8 ± 3.8°	1390°
Trouton's Constant, cal./deg. mole,	21.8	21.6	14.4

strongly suggest that the tellurium vapor is indeed composed primarily of diatomic molecules. These data also show that the values quoted by Yost and Russell[48] are probably incorrect. These values are suspect since they were determined from data obtained in earlier measurements made by the gas-saturation method which yielded values that were inconsistent among the various investigators.

Using the values of vapor pressure calculated by the equation of Brooks,[4]

$$\log P = \frac{-5960.2}{T} + 7.5999, \qquad \text{(IV-3)}$$

where

P = vapor pressure of liquid tellurium, mm., and

T = temperature of liquid tellurium, deg. Kelvin,

the association number was determined for the various tellurium data, and, as expected, the values of the association number were all equal to 2 within the experimental error. It is interesting to note that the values were all slightly higher than 2.00 indicating a possible constant error in the determination. This constant error was probably associated with the analytical determination of the tellurium content of the quartz cell.

Molar Heat of Vaporization, Normal Boiling Point, and Trouton's Constant for Polonium

Several experimental runs were made on three polonium samples. The data obtained for the density of the polonium vapor at various

temperatures and pressures with two polonium samples which contained less than 1 atomic per cent lead impurity are reported in Tables IX and X. The logarithm of the product, (θT_A), was plotted versus the reciprocal of the absolute temperature of the condensed phase in Figure 16. It will be observed that here again, as in the case of the tellurium, although the values of the product (θT_A) were determined for measurements in which the temperature differential, $(T_A - T_B)$, was varied from 40.0° to 474.9° C., all of the data conform to a linear plot within the accuracy of the measurements. The experimental data for the values of the product, (θT_A), obtained at constant pressure are reported in Table XI. These data show that the product, (θT_A), remains constant for large changes in the temperature of the vapor. Thus it appears that polonium vapor is also composed of a single molecular species over the temperature range investigated. The molecular spectrum of polonium, heated to about 400° to 500°C., was studied by G. W. Charles.[49] He obtained several spectograms with well-defined bands of Po_2 molecules. Since these results indicate the presence of diatomic polonium at these temperatures, the assumption, in this investigation, was made that the vapor consists entirely of diatomic polonium molecules. Then, using equation (I-2), the corresponding vapor pressures were calculated from the values of θT_A for the various data. These vapor pressure values are also reported in Tables IX and X. The logarithm of the vapor pressure values was plotted versus the reciprocal of the absolute temperature of the condensed phase. This curve appears in Figure 17. The equation for the

linear curve was then solved by the method of least squares and the standard deviation of the slope and the intercept of the line determined:

$$\log P = \frac{-5749.1 \pm 32.9}{T_B} + 8.4233 \pm 0.0430, \qquad \text{(IV-4)}$$

where

P = vapor pressure of liquid polonium, mm.

T_B = temperature of liquid polonium, deg. Kelvin.

Using the above equation, values for the molar heat of vaporization, normal boiling point, and Trouton's constant were calculated. These values are reported below:

Molar Heat of Vaporization	26.31 ± 0.15 kcals./mole
Normal Boiling Point	946.5° ± 10.2° C.
Trouton's Constant	21.6 cals./deg. mole.

The calculated values of vapor pressure obtained in this investigation were then fitted to the curve determined by Brooks[6] in his studies of the variation of vapor pressure of polonium with temperature using a quartz bourdon gage. This graph is presented in Figure 18. Also, the values for the molar heat of vaporization, normal boiling point, and Trouton's constant as determined in this study are compared with the values calculated by Brooks. These data are reported in Table XVIII.

A comparison of the values in Table XVIII shows variations between the two sets of data which are much greater than could be explained by possible errors in the present investigation. It is believed that the discrepancies are due primarily to the effects of the

TABLE XVIII

Comparison of Values for Heat of Vaporization, Normal Boiling Point, and Trouton's Constant Reported for Polonium

	This Work	Brooks [6]
Heat of Vaporization, kcals. / mole,	26.31 ± 0.15	24.60 ± 0.03
Normal Boiling Point, deg. C.,	946.5° ±10.2°	962.0 ± 1.9°
Trouton's Constant, cal. /deg. mole,	21.6	24.6

decay products and to radiation damage of the quartz used in the determinations.

It will be noted in Figure 18 that the curve for the data obtained in the present study is much lower than the Brooks curve at low vapor pressures, whereas the two curves appear to agree at vapor pressures above 10 mm. This observation suggests that one possible source of error in the direct-pressure measurements could be due to the helium gas produced by the alpha particles. A calculation of the number of alpha particles emitted per day by one curie of polonium shows that 0.00012 cc. of helium gas at standard temperature and pressure, are formed through normal decay. To obtain an indication of the effect of such quantities of gas on measurements made with a quartz bourdon gage, consider a gage of about 10-cc. volume containing approximately 10 curies of polonium. The pressure build-up in the gage due to the helium formed would be about 0.3 mm./day for measurements made at temperatures in the vicinity of 600° C. Thus, relatively large errors are possible in any direct-pressure measurements made at low vapor pressures unless the effect of the helium is taken into consideration; Brooks[6] did not mention any such correction.

In the vapor-density method used in this investigation, the helium produced has very little effect. The only effect would be the depression of vapor pressure due to the external pressure of the inert gas on the liquid phase. Klotz[50] has shown that for small increases in pressure

above a liquid-vapor equilibrium by an inert gas, the change in vapor pressure with increasing pressure on the liquid is given by the following equation:

$$\left(\frac{dP_g}{dP_l}\right)_T = \frac{V_l}{V_g} \qquad \text{(IV-5)}$$

where

dP_g = change in vapor pressure

dP_l = change in pressure on liquid phase due to addition of small quantity of inert gas

V_g = volume of a given weight of substance

V_l = volume of a corresponding weight of liquid.

Because the volume of the vapor for a given weight of polonium is very much greater than the volume of a corresponding weight of polonium liquid, the depression of vapor pressure due to the pressure of the helium produced is several orders of magnitude smaller than the accuracy of the determinations. Therefore, the effect of the helium can be ignored.

The lead is an impurity which is always present in varying amounts in polonium. In order to obtain information as to the magnitude of the error which was introduced in vapor-density or vapor-pressure measurements on polonium by the lead, one polonium sample was studied over a 73-day period. The measurements were taken at periods of 6 to 7 days, 38 to 39 days, and 70 to 73 days following

initial purification of the polonium and sealing of the quartz cell. The lead concentrations corresponding to these periods were 3 to 3.5 atomic per cent, 17 to 17.8 atomic per cent, and 29 to 31 atomic per cent, respectively. The data obtained is tabulated in Tables XII, XIII, and XIV. The logarithm of the product, (θT_A), was plotted versus the reciprocal of the absolute temperature of the condensed phase in Figure 19. The logarithm of the calculated values of vapor pressure versus the reciprocal of the absolute temperature of the condensed phase was plotted in Figure 20. The values of the vapor pressure decreased with increasing lead concentrations as expected. Assuming Raoult's law[51] holds for solutions of lead in liquid polonium, the expected lowering of the vapor pressure for lead concentrations of 0 to 1 atomic per cent, 3 to 3.5 atomic per cent, and 17 to 17.8 atomic per cent was calculated for temperatures of 441.2°, 467.6°, and 496.1°C. For the purpose of these calculations, the vapor pressure of the pure polonium was evaluated graphically by plotting the observed vapor pressures from Figure 20 versus the lead concentration and extrapolating the curve to zero lead content. The values thus obtained were approximately 4 per cent higher than the corresponding values determined for polonium with 0 to 1 atomic per cent lead. The data for the calculated and observed decrease in vapor pressures for the various lead concentrations and temperatures are tabulated in Table XIX. It was found that the observed values for the decrease in vapor pressure were approximately

five times greater than the calculated values. These results suggest that Raoult's law was not obeyed in the lead-polonium solutions, and (or), that the lowering of the vapor pressures was due to other factors besides the lead impurity. One probable cause is considered to be the radiation-attack on the quartz which might result in radiation-induced reactions between the polonium and the quartz. The quartz tube of the quartz cell was inspected at the end of the 73-day period and the inside surface was found to be strongly "crazed" giving an appearance similar to soft glass that has been subjected to a strong thermal shock.

Measurements were made on the three polonium samples (containing different initial amounts of polonium) when their lead concentration was 3 to 3.5 atomic per cent. These data are reported in Tables XII, XV, and XVI. The logarithm of the calculated vapor pressures for these data was plotted versus the reciprocal of the absolute temperature of the condensed phase in Figure 21. This graph also includes the curve for the polonium-vapor pressures determined from polonium samples with less than one atomic per cent lead impurity. An examination of this graph shows that the three curves for the samples of polonium containing 3 to 3.5 atomic per cent lead impurity are similar for vapor pressures below 1.5 mm. and then tail-off in similar manners at different vapor pressures above 1.5 mm. Furthermore, the slope of the straight-line portions of these curves is slightly smaller than the slope of the curve for the polonium with 0 to 1 atomic

TABLE XIX

Comparison of Calculated and Observed Values for the Decrease in Vapor Pressure of Polonium by Different Lead Concentrations

Pb conc., atomic per cent	Decrease in Vapor Pressure, mm. at 441.2°C. obs.	calc.	at 467.6°C. obs.	calc.	at 496.1°C. obs.	calc.
0 to 1	.018	.003	.03	.006	.07	.014
3 to 3.5	.058	.014	.10	.026	.30	.058
17 to 17.8	.240	.072	.45	.13	.88	.28

per cent lead. These are the results one would expect if the lead is non-volatile and soluble in the molten polonium over the temperature range studied. At very low vapor pressures, only a small fraction of the polonium in the cell is in the vapor state so the concentration of the lead in the molten polonium is essentially the same for all three samples. As the temperature of the condensed phase is increased, the amount of polonium vaporized per degree increases with the result that the concentration of the non-volatile lead in the remaining molten polonium increases causing the slope of the line to decrease relative to the 0 to 1 atomic per cent lead curve. For the polonium sample containing the smaller initial quantity of polonium, the point is soon reached at which the lead concentration is increasing very rapidly with small increases in the temperature of the condensed phase. This results in the tailing-off of the vapor-pressure curve. This tailing-off occurs in a similar manner for the other two samples, but because of the higher initial polonium content, higher values of vapor pressures are required before the lead concentration in the liquid polonium is high enough to cause the curves to tail-off. Thus, these curves suggest that the lead is soluble in the polonium and does not form a volatile compound. These results are in accord with the findings of Witteman, Giorgi, and Vier[26] in their studies on the preparation and structure of the intermetallic lead polonide compound.

The association numbers, α, were determined for the various

polonium data from values of vapor pressures calculated by the equation of Brooks:[6]

$$\log P = \frac{-5377.8}{T} + 7.2345, \qquad \text{(IV-6)}$$

where

P = vapor pressure of liquid polonium, mm.

T = temperature of liquid polonium, deg. Kelvin.

The values of the calculated association numbers were found to vary from 1.38 to 1.75 with the values increasing as the vapor pressure in the system increased. It is believed that these variations in the association numbers are due to errors inherent in the two investigations as previously described and not the result of any dissociation. This belief is based on the following arguments:

(1) the values for the product, (θT_A) at constant pressure were constant for the variations in the temperature differential, $(T_A - T_B)$, from 60.1° to 474.9° C.: if a dissociation equilibrium existed in the polonium vapor, the values of θT_A should have decreased with increasing vapor temperature,

(2) in the plot of log (θT_A) versus the reciprocal of the absolute temperature of the condensed phase, the values of θT_A for the measurements taken in which the temperature differential, $(T_A - T_B)$, was above 50°C. should have fallen below the line fitted to the data for measurements taken with the temperature differential below 50°C.; however, all of the data fitted to the

same straight-line curve within the accuracy of the measurements,

(3) consideration of Figure 18 shows that the Brooks curve and the curve which represents the data from this investigation approach each other at the higher temperatures. This behavior is opposite to what would be expected if any dissociation equilibria existed in the polonium vapor.

On the basis of the above arguments, the results of this investigation suggest that polonium vapor consist primarily of diatomic molecules over the temperature range studied, 422° to 1013° C.

Conclusion

The results of this investigation suggest that both tellurium and polonium vapor consist primarily of diatomic molecules over the temperature range studied, from 512° to 880° C. for tellurium and from 422° to 1013° C. for polonium. The selenium vapor appears to contain several molecular species including one form which is greater than Se_6.

The vapor density method shows great promise for use with systems of low vapor pressures at elevated temperatures. For example, if the quartz cell is replaced with an iridium or tantalum tube, measurements can readily be made at temperatures in excess of 2000° C. Furthermore, several measurements over wide changes in pressure and temperature are possible with one sample.

The usefulness of this method at temperatures below 1200° C.

could be extended by constructing the quartz cell in the form of a quartz bourdon gage so that simultaneous measurements of pressure and vapor density could be made on samples over wide ranges of temperature and pressure. This would provide a convenient method for studying various dissociation equilibria at elevated temperatures.

BIBLIOGRAPHY

1. J. J. Doolan and J. R. Partington, Faraday Soc., 20, 342 (1924).
2. A. Schneider and K. Schupp, Z. Electrochem., 50, 163 (1944).
3. K. Niawa and Z. Sibata, J. Faculty Sci., Hokkaido Imp. Univ., 61, 667 (1940), C. A., 34, 7681 (1940).
4. L. S. Brooks, J. Am. Chem. Soc., 74, 227 (1952).
5. D. M. Yost and H. R. Russell, Systematic Inorganic Chemistry, Prentice-Hall, Inc., New York, 1944, p. 285.
6. L. S. Brooks, J. Am. Chem Soc., 77, 3211 (1955).
7. J. R. Partington, An Advanced Treatise on Physical Chemistry, Longman, Green and Co., New York, 1949, p. 758.
8. J. R. Partington, op. cit., p. 760.
9. J. R. Partington, op. cit., p. 762.
10. E. Sommaruga, Ann., 195, 302 (1879).
11. A. Magnus and E. Schmid, Z. anorg. chem., 120, 232 (1922).
12. W. Ramsay and S. Young, Phil. Trans., 178, 57 (1887).
13. P. Blackman, J. Phys. Chem., 13, 138 (1909).
14. G. L. Matheson and O. Moass, J. Am. Chem. Soc., 51, 674 (1929).
15. A. S. Coolidge, J. Am. Chem. Soc., 50, 2166 (1928).
16. P. A. Giguere and R. E. Rudle, J. Am. Chem. Soc., 63, 1135 (1941).
17. D. A. Peak and R. A. Robinson, J. Phys. Chem., 38, 941 (1934).
18. J. B. Niederl, Z. anal. Chem., 77, 169 (1929).
19. V. Meyer and J. Mensching, Z. phys. Chem., 1, 145 (1887).
20. W. Nernst, Z. Elektrochem., 9, 622 (1903).
21. H. von Wartenberg, Z. anorg. Chem., 56, 320 (1908).

22. F. S. Dainton and H. M. Kimberley, Trans. Faraday. Soc., 46, 912 (1950).

23. C. Barthel and M. Dode, Bull. soc. chim. France, 21, 1312 (1954).

24. I. M. Klotz, Chemical Thermodynamics, Prentice-Hall, Inc., New York, 1950, pp. 136-137.

25. W. H. Beamer and C. R. Maxwell, J. Chem. Phys., 17, 1293 (1949).

26. W. G. Witteman, A. L. Giorgi, and D. T. Vier, Los Alamos Scientific Laboratory Report LA-1890, March 1955.

27. R. Krohn, personal communication.

28. M. G. Bowman and N. H. Krikorian, Los Alamos Scientific Laboratory Report LA-1402, February 1952. (Classified)

29. G. N. Rupert, Los Alamos Scientific Laboratory Report LA-1486, December, 1952.

30. R. K. Money and M. G. Bowman, Los Alamos Scientific Laboratory Report LA-1401, February 1953. (Classified)

31. M. G. Bowman and N. H. Krikorian, op. cit., p. 17.

32. C. V. Kent and J. M. Cook, Phys. Rev., 61, 389 (1942).

33. W. R. Meyer, Plating and Finishing Guidebook, 10th ed., The Metal Industry Publishing Co., Inc., New York, 1941, p. 31.

34. W. F. Hillebrand and G. E. F. Lundell, Applied Inorganic Analysis, John Wiley and Sons, Inc., New York, 1953, pp. 337-338.

35. C. V. Kent and J. M. Cook, Phys. Rev., 62, 297 (1942).

36. A. G. Gray, Modern Electroplating, John Wiley and Sons, Inc., New York, 1953, p. 487.

37. W. R. Schoeller, Analyst, 64, 318 (1939).

38. W. F. Hillebrand and G. E. F. Lundell, op. cit., p. 334.

39. W. F. Hillebrand and G. E. F. Lundell, op. cit., pp. 189 and 196.

40. W. F. Hillebrand and G. E. F. Lundell, op. cit., p. 197.

41. W. B. Lewis and B. V. Bowden, Proc. Roy. Soc., London, A145, 235 (1934).

42. J. Grant, Sutton's Volumetric Analysis, 13th ed., Butterworths Scientific Publications, London, 1955, p. 443.

43. W. C. Coleman and C. R. McCrosky, Anal. Ed., 9, 431 (1937).

44. W. E. Deming, Statistical Adjustment of Data, John Wiley and Sons, Inc., New York, 1943, p. 173.

45. W. E. Deming, op. cit., p. 168.

46. G. Preuner and W. Schupp, Z. physik. Chem., 81, 129 (1912).

47. D. M. Yost and H. R. Russell, op. cit., p. 285.

48. D. M. Yost and H. R. Russell, op. cit., p. 285.

49. H. V. Moyer, Polonium, Office of Technical Services, Department of Commerce, Washington, D. C., 1956, pp. 30-31.

50. I. M. Klotz, op. cit., pp. 137-138.

51. I. M. Klotz, op. cit., p. 258.